Journal of Medicinal Chemistry

pubs.acs.org/jmc

Article

Discovery and Optimization of a STING Agonist Platform for Application in Antibody Drug Conjugates

Jeremy R. Duvall,* Joshua D. Thomas, Raghida A. Bukhalid, Kalli C. Catcott, Keith W. Bentley, Scott D. Collins, Timothy Eitas, Brian D. Jones, Eugene W. Kelleher, Kelly Lancaster, Marina Protopopova, Soumya S. Ray, Elena Ter-Ovanesyan, Ling Xu, Liping Yang, Jeffrey Zurita, Marc Damelin, Dorin Toader, and Timothy B. Lowinger

Cite This: *J. Med. Chem.* 2023, 66, 10715−10733

Read Online

ACCESS | Metrics & More | Article Recommendations | Supporting Information

ABSTRACT: While STING agonists have proven to be effective preclinically as anti-tumor agents, these promising results have yet to be translated in the clinic. A STING agonist antibody−drug conjugate (ADC) could overcome current limitations by improving tumor accessibility, allowing for systemic administration as well as tumor-localized activation of STING for greater anti-tumor activity and better tolerability. In line with this effort, a STING agonist ADC platform was identified through systematic optimization of the payload, linker, and scaffold based on multiple factors including potency and specificity in both in vitro and in vivo evaluations. The platform employs a potent non-cyclic dinucleotide STING agonist, a cleavable ester-based linker, and a hydrophilic PEG8-bisglucamine scaffold. A tumor-targeted ADC built with the resulting STING agonist platform induced robust and durable anti-tumor activity and demonstrated high stability and favorable pharmacokinetics in nonclinical species.

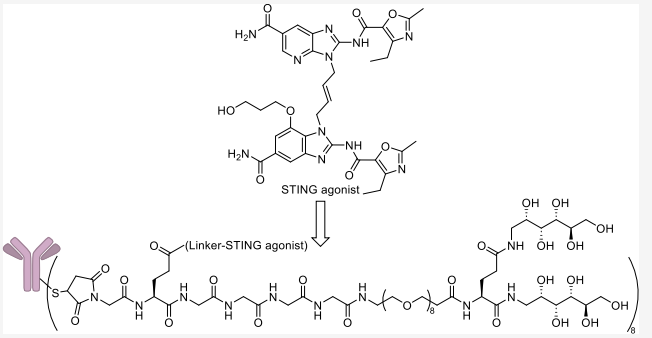

INTRODUCTION

Novel cancer immunotherapies, such as checkpoint inhibitors, have proven to be a vital approach for the treatment of an increasing number of cancers. While these therapies successfully modulate the immune system to eradicate metastases, their success does not translate well to "cold" or "non-T cell-inflamed" tumors that lack sufficient T cell infiltrates or exhibit immune suppression prior to treatment.[1,2] One approach to overcome this resistance is to activate the innate immune system via known signaling pathways, including toll-like receptor (TLR) 7/8, nucleotide-binding oligomerization domain, and cGAS-STING.[3,4] STING agonism has been shown pre-clinically to have enormous potential as an anti-cancer therapeutic approach using the natural agonist, cGAMP (**1**, Figure 1) or other cyclic dinucleotide (CDN) derivatives (exemplified with ADU-S100, **2**, Figure 1).[5] Although CDNs have been mostly limited to intratumoral administration routes, non-CDN STING agonists have been identified, such as dimeric amidobenzimidazole (diABZI, exemplified with **3**, Figure 1),[6] with demonstrated anti-tumor activity preclinically after systemic administration. However, this exciting potential has yet to be realized in the clinic, possibly due to the limitations of historic STING agonist delivery strategies.[7]

Antibody−drug conjugates (ADCs) serve as a powerful paradigm for systemic, yet targeted, delivery of small-molecule "drugs" (also referred to as payloads) aimed at minimizing systemic exposure of the active agents. ADCs are typically made up of 3 key components—antibody, payload, and the linker connecting the two. The antibody targets an antigen that is preferentially overexpressed on cancer cells and acts as a delivery mechanism, localizing the ADC to the tumor and providing active delivery of the payload into the desired cell type within the tumor microenvironment. The linker is designed to be stable in circulation but to efficiently release the payload upon internalization of the ADC into the target cell. The chosen payload does not typically elicit a biological response while attached to the antibody and only becomes functionally active once released from the ADC, completing the strategy of localizing the activity of the payload to the targeted cell. ADCs to date have predominantly been equipped with cytotoxic payloads, but recently, a new generation of payloads have been reported within the ADC field, including protein degraders,[8] TLR agonists,[9−11] and other payload classes for non-oncology indications.[12,13] We hypothesized that

Received: May 19, 2023
Published: July 24, 2023

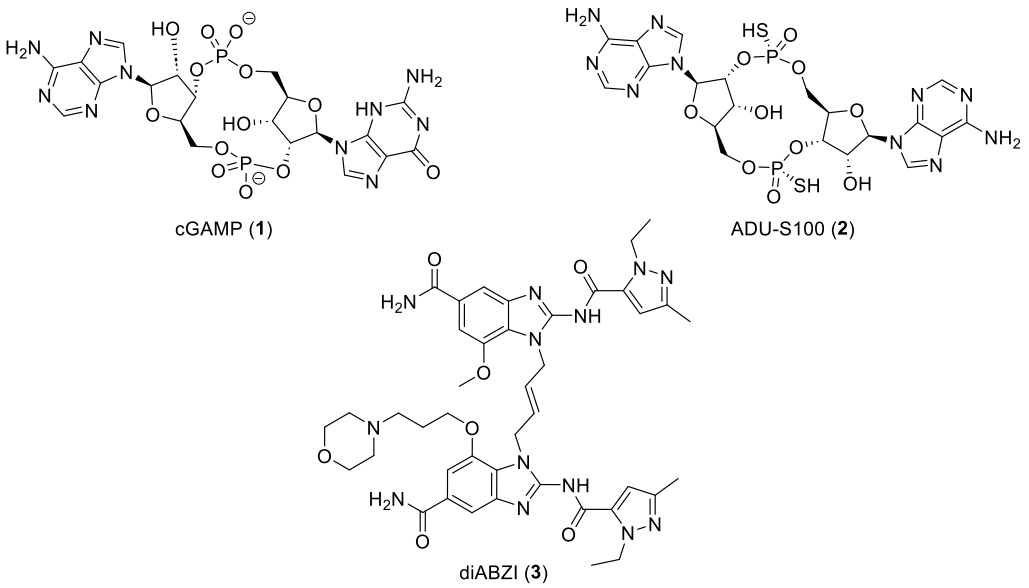

Figure 1. Examples of natural and synthetic STING agonists.

an ADC strategy could be applied to STING agonists, overcoming some of the current limitations through (1) targeted delivery, thereby increasing efficacy and reducing toxicity; (2) improved pharmacokinetics; and (3) accessibility to metastatic sites and not only injectable lesions, with no restriction on tumor type, location, or size.

Our approach to develop a STING agonist ADC started with building the optimal platform (historically referred to as the "drug-linker"), which would result in desired drug-like properties and performance. When designing the platform, we considered three main components: payload, scaffold (molecular feature designed to improve the biophysical properties of the ADC), and linker (which connects payload to scaffold). The platform also contains a reactive group that is amenable to various bioconjugation methods for attachment to the antibody. With a focus on the end result, criteria for a successful platform would leave the corresponding ADC with good stability in circulation resulting in high exposure levels, robust anti-tumor activity in vivo with minimal target-independent activity, and a meaningful safety profile. Herein, we describe our approach to developing a STING agonist platform in which we focused on optimizing each of the three components (payload, linker, and scaffold). We conducted the platform optimization using an antibody to the clinically validated target HER2.[14]

RESULTS AND DISCUSSION

Payload Optimization. For the payload component, we purposefully optimized the STING agonist specifically for an ADC approach. Contrary to traditional medicinal chemistry approaches, designing a compound for ADC delivery presents unique challenges. We hypothesized that certain characteristics previously described for traditional, cytotoxic payloads would hold true for a STING agonist payload. For example, considering the amount of the payload delivered to the tumor by an ADC,[15−17] we aimed for a compound that was highly potent. Additionally, we sought a more hydrophilic payload in order to impart favorable pharmacokinetic (PK) properties to the resulting ADC.[18] However, contrary to many cytotoxic ADCs, we also hypothesized that a bystander effect (the ability for the payload to enter neighboring cells once released from the ADC) was not required for an effective response with a STING agonist ADC due to the role of the immune system in the anti-tumor activity (rather than direct killing of the cancer cell by the payload). As such, we believed that low passive permeability would be a desired feature to limit non-targeted tissue uptake. Additionally, if the payload was released prematurely, the compound was designed to be quickly cleared to prevent off-target toxicity, although stable enough to survive the endosomal−lysosomal processing of the ADC (the process by which the payload is released). Finally, the compound needs a site for linker attachment.

Upon evaluating STING agonists for ADC development, a deliberate choice was made to avoid CDNs. Although hydrophilic in nature, CDNs present several challenges such as potential stability liabilities during the endosomal−lysosomal processing of the ADC and the complexities around the synthesis of CDNs and their associated ADCs. As such, the non-CDN STING agonist **3** (Figure 1) served as a good starting point due to the reported potency of the compound. We hypothesized that increasing the hydrophilicity of the compound would improve the overall ADC properties while also giving the desired low passive permeability properties. It was also important to incorporate a functional group for linker attachment in such a way that the biological activity was not adversely affected.

In general, compounds were tested for STING activation utilizing monocytic THP1 interferon regulatory factor 3 (IRF3) reporter cells (InvivoGen) where luciferase transcription is induced upon nuclear translocation of the IRF3 transcription factor following stimulation with STING agonists. The cells were permeabilized using digitonin to avoid false negatives due to poor cell permeability, which could limit prioritization of a payload for ADC delivery where passive permeability is not required. As an orthogonal assay, surface plasmon resonance (SPR) analysis confirmed ligand binding affinity to STING and was consistent with the functional activity observed in the cellular assay (see Table S1 in the Supporting Information). Initial optimization efforts focused on incorporation of a functional group for linker attachment.

https://doi.org/10.1021/acs.jmedchem.3c00907
J. Med. Chem. 2023, 66, 10715−10733

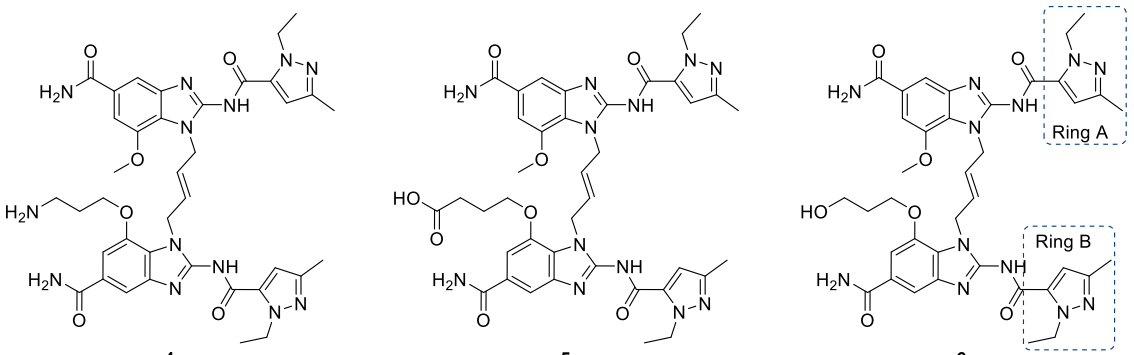

Figure 2. Incorporation of a functional handle for linker attachment.

Table 1. STING Activity with Analogs 6−17

Cmpd	Ring A	Ring B	cLogP	EC_{50} (μM)	Cmpd	Ring A	Ring B	cLogP	EC_{50} (μM)	Cmpd	Ring A	Ring B	cLogP	EC_{50} (μM)
6	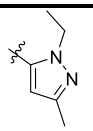	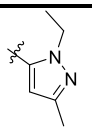	1.58	0.001	**10**	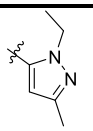	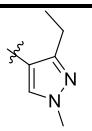	1.24	0.02	**14**	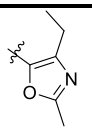	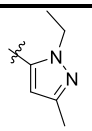	1.21	0.009
7		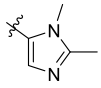	0.79	>100	**11**	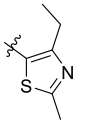	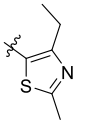	3.02	0.27	**15**	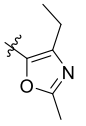	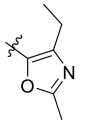	0.83	0.001
8	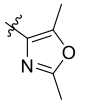	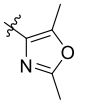	0.48	>100	**12**	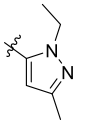	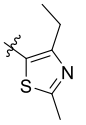	2.52	0.02	**16**			-0.08	>100
9	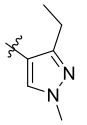	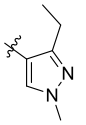	0.90	5.0	**13**	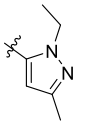	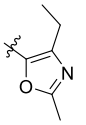	1.21	0.001	**17**	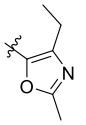	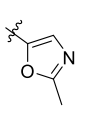	0.38	>100

Based on reported crystal structures,[6,19,20] we hypothesized that the morpholino group could be substituted for other functional groups without greatly affecting the key interactions of the ligand with the STING protein. Satisfyingly, preparation and testing of the corresponding amine **4**, carboxylic acid **5**, and alcohol **6** resulted in active STING agonists that also carry a functional handle for linker attachment (Figure 2). Due to the low nM potency of payload **6**, it was prioritized for subsequent optimization of the heterocyclic amide groups (identified as ring A and ring B) and the benzimidazole scaffold.

Exploration of the heterocyclic amide groups focused on identifying a more hydrophilic ring system that maintained STING agonist activity (Table 1). As an assessment of desired hydrophilicity, the cLog*P* values are included in the table. More polar building blocks (**7** and **8**) were explored but found to be detrimental for activity. Even subtle modifications such as heteroatom placement (**9**) had a substantial negative effect on activity. The loss in activity could be offset by maintaining one of the rings as the parent pyrazole (**10**) but a major breakthrough was the identification of the thiazole ring in **11**. Although detrimental to the hydrophilicity profile and >100-fold less active than **6**, both could be offset by maintaining the pyrazole as one of the rings (**12**). More importantly, the result led to the oxazole ring in **13**, which gave improved hydrophilicity while retaining activity. Flipping the heterocycle ring placement (**14**) did not have a major impact and substituting both heterocycles to the oxazole (**15**) retained the potency, giving us confidence that the oxazole was nearly interchangeable with the pyrazole while being more hydrophilic. The ring substituents remained critical for activity as exemplified by loss of activity with **16**, which could not be reversed even through maintaining one of the active oxazole rings (**17**).

The improved physicochemical properties of compound **15** enabled the co-crystal structure with the STING protein (Figure 3A). The ligand was bound at the interface of the homodimer STING complex. Importantly, the STING complex was in a closed, or active, conformation, contrary to what was reported previously for the diABZI STING agonist class.[6] The difference in binding conformation could be due to the high binding affinity of **15** compared to the published diABZI agonist which was co-crystalized previously. Analysis of the ligand within the binding pocket (Figure 3B) identified two potential areas that could be exploited within the optimization campaign. First, the imidazole double bond of the benzimidazole prefers to be exocyclic rather than the more common endocyclic; and second, a $\pi-\pi$ stacking interaction

https://doi.org/10.1021/acs.jmedchem.3c00907
J. Med. Chem. 2023, 66, 10715−10733

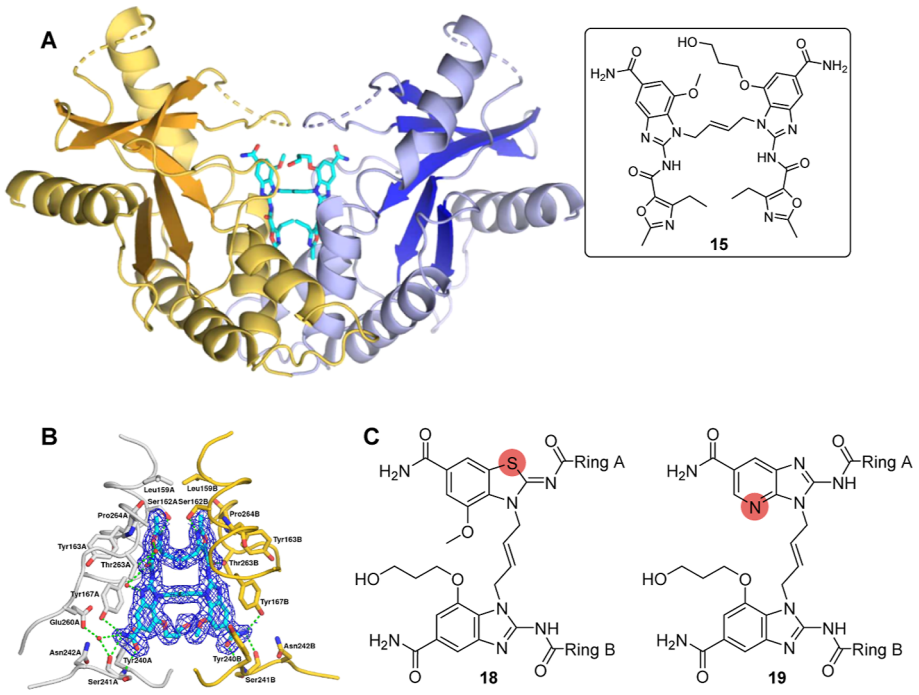

Figure 3. (A) Co-crystal structure of human STING with **15** (PDB ID 8STH) and the 2-D structure of **15** drawn in a similar conformation as observed in the co-crystal structure. (B) Close-up of **15**-STING complex depicting key interactions. (C) Second-generation scaffolds based on the crystal structure.

Scheme 1. Synthesis of Second-Generation Scaffolds 18 and 19[a]

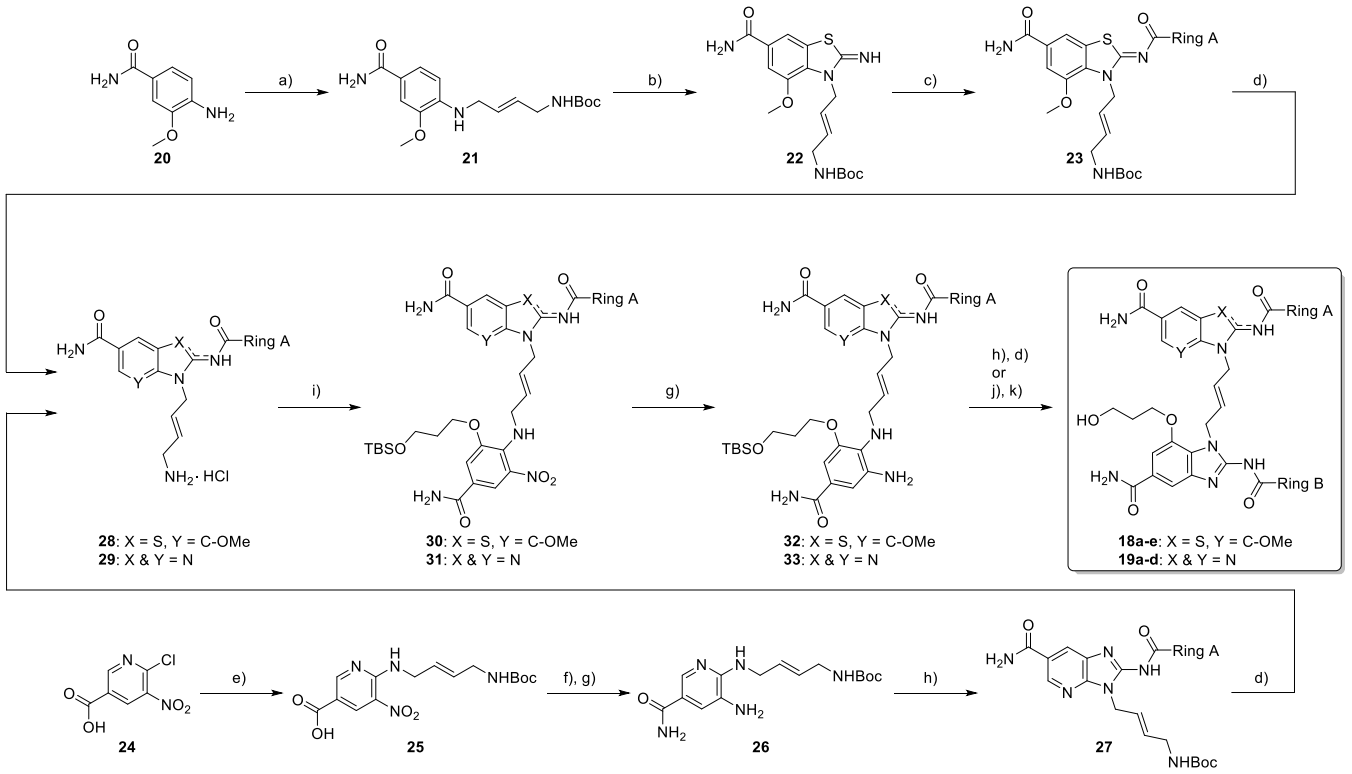

[a]Reagents and conditions: (a) *tert*-butyl *E*-(4-bromobut-2-en-1-yl)carbamate, K_2CO_3, DMF; (b) KSCN, Br_2, AcOH; (c) R−CO_2H, HATU, DIPEA, DMF; (d) HCl, dioxane; (e) *tert*-butyl *E*-(4-aminobut-2-en-1-yl)carbamate, K_2CO_3, DMSO; (f) NH_4Cl, DIPEA, HATU, DMF; (g) $Na_2S_2O_4$, NH_4OH, MeOH, H_2O; (h) R-carbonyl isothiocyanate, EDC, NEt_3, DMF; (i) 3-(3 ((*tert*-butyldimethylsilyl)oxy)propoxy)-4-chloro-5-nitrobenzamide, NEt_3, DMSO; (j) BrCN, MeOH; (k) R−CO_2H, PyBOP, DIPEA, DMF.

exists between the benzimidazole and Tyr167. We imagined that analogs that lock the compound in the preferred conformation (**18**, Figure 3C) or enhance the $\pi-\pi$ interaction (**19**) could result in improved activity or hydrophilicity.

https://doi.org/10.1021/acs.jmedchem.3c00907
J. Med. Chem. 2023, 66, 10715−10733

Synthesis of compounds **18** and **19** leveraged a similar route as that reported[6,21] for the parent benzimidazole series, with a modification in the sequence to allow for "ring A" and "ring B" to be independent of each other (Scheme 1). Synthesis of benzothiazole **18** started with alkylation of aniline **20**, which set up a key cyclization using potassium thiocyanate to give benzothiazole **22**. Subsequent amidation completed the northern heterocycle amide motif. The remaining synthetic approach to complete analogs **18a−d** was similar to that reported. Synthesis of the azabenzimidazole **19** started with a S_NAr reaction with pyridine **24**, followed by reduction of the nitro group to give cyclization precursor **26**. Treatment with an isothiocyanate generated azabenzimidazole **27** with the heterocyclic amide installed. Like the benzothiophene route, the azabenzimidazole was completed through a 5-step sequence including Boc deprotection, S_NAr reaction, reduction, and cyclization/amidation. Typically, cyclization with BrCN resulted in TBS deprotection, which could remain unprotected through the final amidation step.

The newly generated analogs were assessed for STING activation in permeabilized THP1 cells (Table 2). Indeed, the benzothiazole motif was tolerated, with compounds **18a** and **18b** showing good STING agonist activity, although there was a preference for the pyrazole building block (**18a**) as the oxazole analog (**18b**) showed ∼10-fold weaker activity. Similar results were observed with the steep structure−activity relationship of the heterocycle, with even an ethyl to methyl group switch (**18c** versus **18d**) or removal of a methyl group (**18e**) not being tolerated. Since there was no improvement in activity and with the expected loss in hydrophilicity, the benzothiazole series was deprioritized. Satisfyingly, the azabenzimidazole compounds also showed good activity, but in this case, oxazole analog **19b** showed 10-fold better activity than pyrazole analog **19a** while also having improved hydrophilicity. Similar changes in the heterocycle amide had a detrimental effect on STING agonist activity (**19d**) and no improvement was seen with the mixed heterocycle analog **19c**. Additional analogs which were hybrids of the benzothiazole scaffold and the azabenzimidazole scaffold were generated, including azabenzathiazole **34**, but they were not found to present any advantages over the analogs already in hand (Figure 4). With **19b** showing the best profile of activity and hydrophilicity, further characterization was completed including activity in human white blood cells, cross-species STING binding and activation, off-target activity, cell permeability, metabolism, and in vivo PK (see ref 14 and Table S2 in the Supporting Information). Additionally, co-crystal structure determination confirmed that **19b** bound in a similar way as that of **15**, with the ligand binding at the interface of the homodimer STING complex and the complex was in a closed confirmation (see Figure S1 in the Supporting Information). Based on the totality of the data package, compound **19b** was selected as the lead payload for ADC platform development.

Linker Optimization. The second step in identifying an optimal STING agonist platform was to determine the correct linker to covalently attach the payload to the scaffold. Although options are broadly categorized into cleavable and non-cleavable linkers, there are several different functional groups and/or trigger points that can be used for either category of linkers. In a data-driven approach, several linkers were explored representing both cleavable and non-cleavable formats to determine the optimal choice for delivering a STING agonist via an ADC. In evaluating the different linkers, the corresponding ADCs were assessed for their analytical properties [hydrophobic interaction chromatography (HIC) and size exclusion chromatography (SEC)], in vitro activity, in

Table 2. STING Activity with Analogs 18a−e and 19a−d

	Cmpd	Ring A	Ring B	cLogP	EC_{50} (μM)
Benzothiazole Series	18a	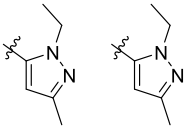		4.19	0.005
	18b	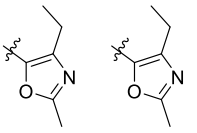		4.11	0.06
	18c	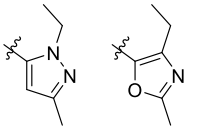		4.04	0.02
	18d	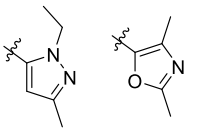		3.51	>100
	18e	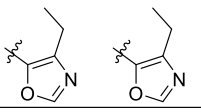		3.11	>100
Azabenzimidazole Series	19a	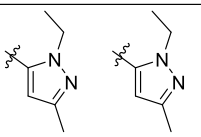		0.67	0.06
	19b	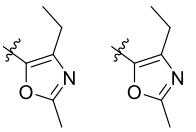		-0.17	0.007
	19c	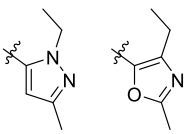		0.29	0.004
	19d	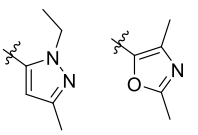		-0.23	3.2

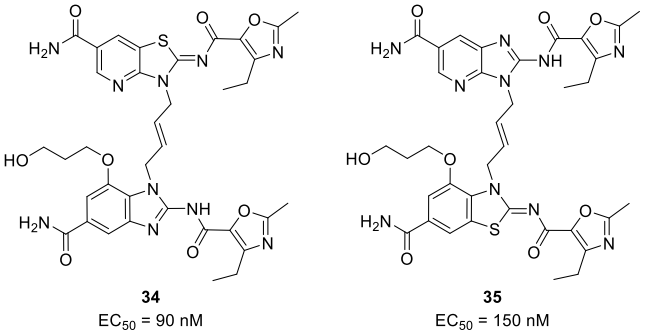

34
EC_{50} = 90 nM

35
EC_{50} = 150 nM

Figure 4. Additional scaffold variants with STING agonist activity.

https://doi.org/10.1021/acs.jmedchem.3c00907
J. Med. Chem. 2023, 66, 10715−10733

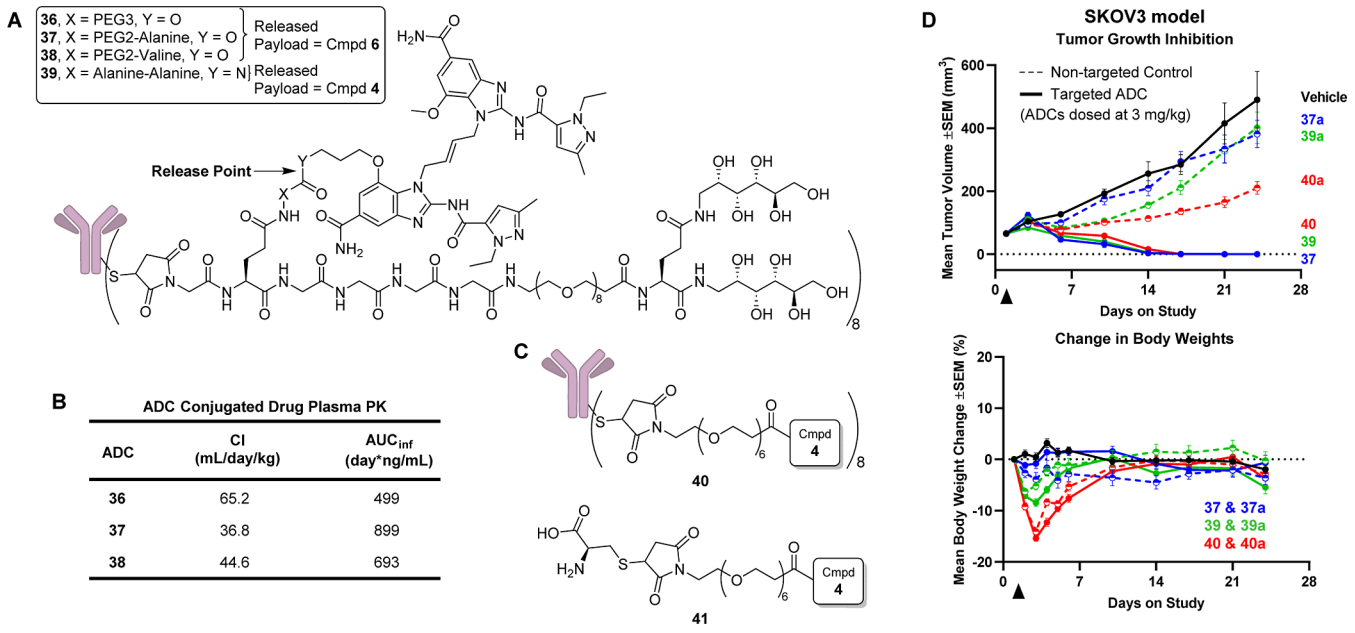

Figure 5. Evaluation of lead linkers using trastuzumab-based ADCs. (A) Structures of cleavable linkers. (B) In vivo mouse plasma PK analysis for the conjugated drug of ADCs with a cleavable ester linker. (C) Structure of non-cleavable linker **40** and the released payload **41**. (D) In vivo comparison of tumor growth inhibition and changes in body weight loss of different cleavable and non-cleavable linkers in a SKOV3 xenograft model. Doses were matched by antibody at 3 mg/kg.

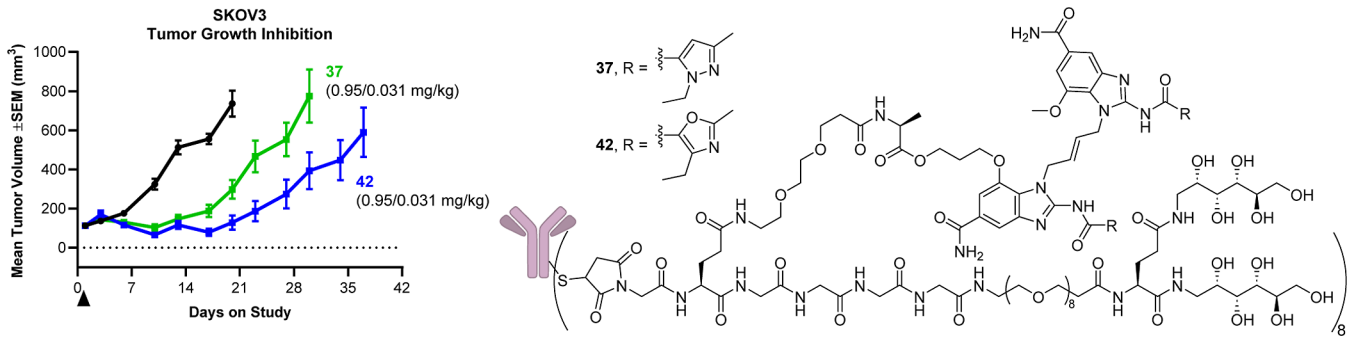

Figure 6. In vivo anti-tumor activity in a SKOV3 xenograft model comparing payloads varying in hydrophilicity with HER2-targeted HT-19-based ADCs. Dose levels are shown by antibody/payload and were chosen at a sub-optimal level to allow for differentiation between test articles.

vivo PK, anti-tumor activity, and impact on off-target activity. Other parameters, such as payload and antibody, were held constant as the linker was evaluated.

In an attempt to assess the best possible linker from each respective class, several criteria were considered. For example, an ester attachment is known to be susceptible to potential metabolism, as exemplified by ADC **36** (Figure 5A), which has an unhindered ester bond. Addition of an alanine adjacent to the ester bond resulted in more stable ADC **37** and nearly 2-fold improvement in exposure of the conjugated drug (Figure 5B). However, even more hindered amino acids, such as the valine in ADC **38**, did not result in an improved PK profile compared to **37**. Whereas ADCs **36**−**38** leverage **6** as the payload, ADC **39**, which employs a cleavable peptide-based linker, uses **4** as the payload. For assessing the non-cleavable linker, the scaffold, which attenuates the biophysical properties of the ADC, was removed as it was expected to detrimentally impact the activity of the released payload due to its large size (Figure 5C). Activity of the anticipated released payload **41** (Figure 5C) from ADC **40** was tested and confirmed to be similar to the payload released from **37** (payload **6**), with similar binding (as assessed by SPR, see Table S1 in the Supporting Information) and an EC_{50} value of 5 nM in the permeabilized THP1 cell assay. Although **40** was more hydrophobic (as assessed by HIC, see Figure S2 in the Supporting Information) compared to **37** and **39**, it was expected to be sufficient to evaluate the non-cleavable linker in vivo.

The three trastuzumab-based (HER2-targeted) ADCs were evaluated for in vivo anti-tumor activity after a single dose of 3 mg/kg (~0.1 mg/kg by payload) administered intravenously (Figure 5D). Additionally, non-targeting isotype controls (**37a**, **39a**, and **40a**) were generated by conjugating each platform to a non-targeting antibody (palivizumab) and assessed at the same dose. Satisfyingly, all 3 targeted ADCs showed excellent anti-tumor activity with complete and durable tumor regressions observed for all animals. However, the non-targeting isotype controls did show differentiation, with target-independent activity being observed for **40a** (employing the non-cleavable linker) and, to a lesser extent, **39a** (employing the cleavable peptide linker). This was associated with body weight loss for both targeted and non-targeted

https://doi.org/10.1021/acs.jmedchem.3c00907
J. Med. Chem. 2023, 66, 10715−10733

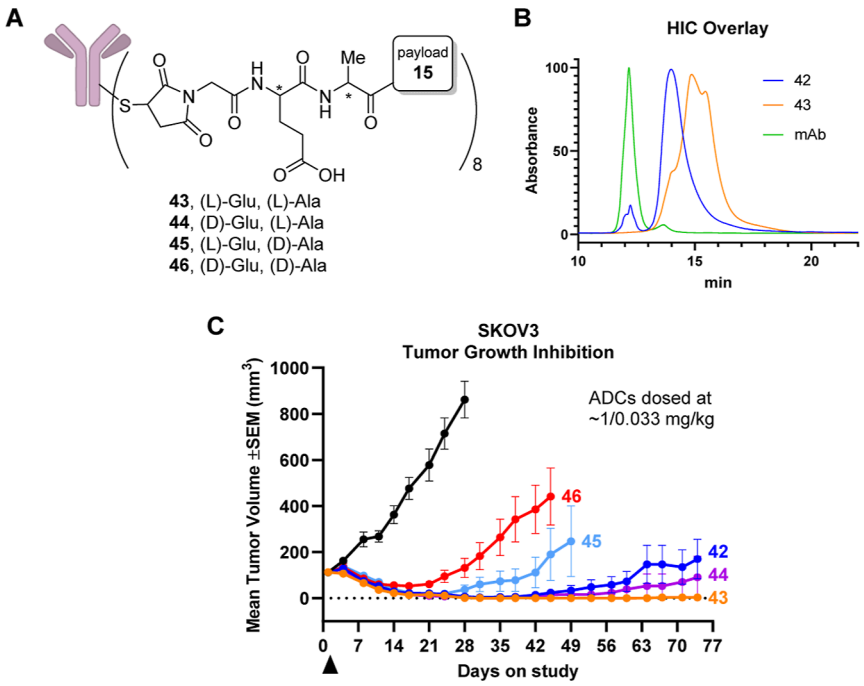

Figure 7. (A) Structures of low-MW scaffolds. (B) HIC overlay comparing ADCs using the low-MW scaffold and PEG8-bisglucamine scaffold versus free antibody. (C) In vivo anti-tumor activity in a SKOV3 xenograft model comparing various low-MW scaffolds at a matched dose level of 0.033 mg/kg by payload.

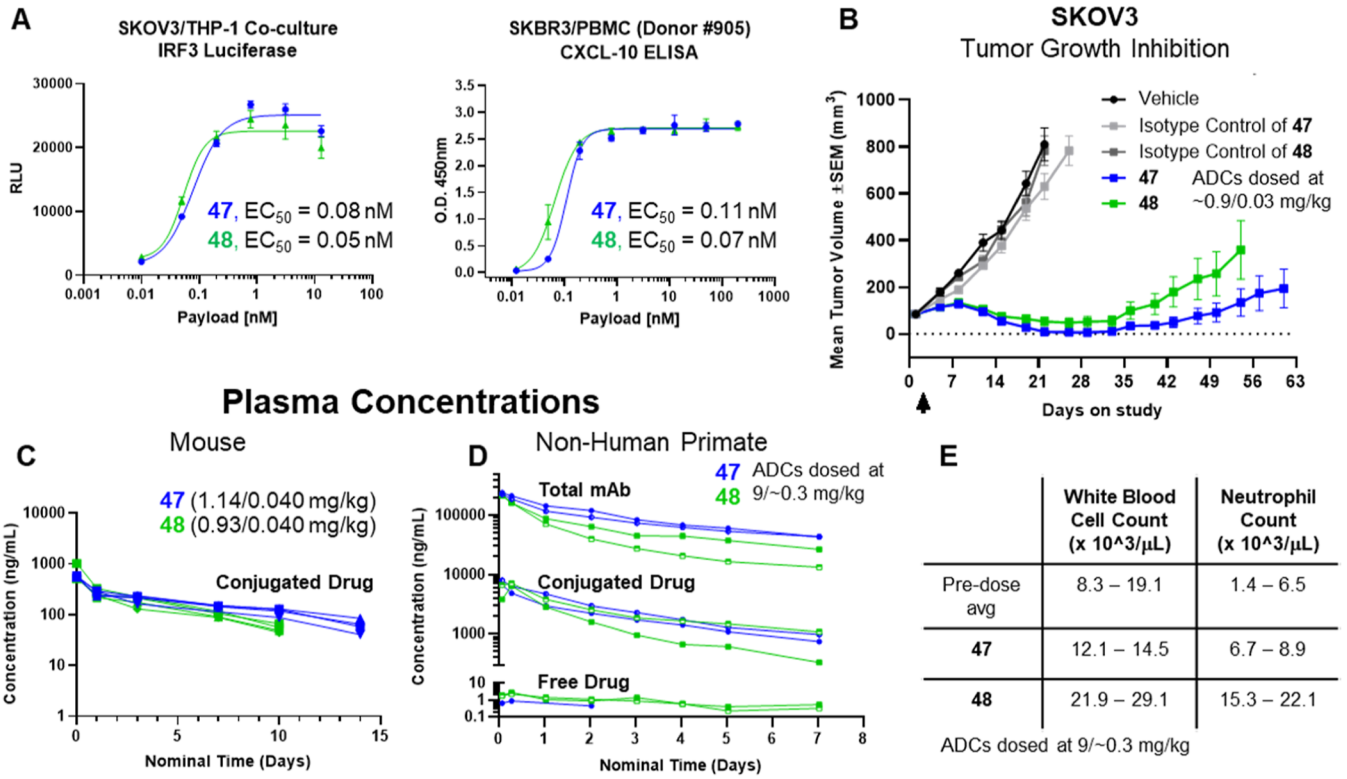

	White Blood Cell Count (x 10^3/μL)	Neutrophil Count (x 10^3/μL)
Pre-dose avg	8.3 – 19.1	1.4 – 6.5
47	12.1 – 14.5	6.7 – 8.9
48	21.9 – 29.1	15.3 – 22.1

Figure 8. Comparison of PEG8-bisglucamine scaffold and optimal low-MW scaffold with lead payload **19b**. (A) Activity in in vitro co-culture assays. (B) Anti-tumor activity in a SKOV3 xenograft model. In vivo PK in (C) mouse and (D) non-human primate. (E) Key hematology parameters at 24 h post dose in non-human primates. For (B–E), dose levels are shown by antibody/payload. For (C,D), conjugated drug refers to the parameter measuring drug conjugated to the antibody representative of ADC exposure; the multiple lines represent individual animals within the studies.

ADCs. ADC **37**, employing the ester cleavable linker, showed similar effects on body weight levels as mice administered vehicle and showed no activity in its corresponding non-binding control **37a**. Based on these data, the ester cleavable linker was prioritized for the STING agonist platform.

https://doi.org/10.1021/acs.jmedchem.3c00907
J. Med. Chem. 2023, 66, 10715–10733

Scaffold Optimization. With an optimal linker in hand, scaffold optimization was pursued next. At this stage of the project, the antibody was switched from trastuzumab to HT-19, a HER2-targeted antibody specifically developed for use in an ADC.[14] Initial efforts focused on using **6** as the payload and as such, a more hydrophilic scaffold that included the PEG8-bisglucamine motif in **37** (Figure 5A) was needed. Additional design components for the starting scaffold included the self-hydrolyzing maleimide motif,[22] a branching point that positions the hydrophilic group adjacent to the payload,[23,24] and placing the payload closer to the mAb,[25] all of which have been shown to generally improve the stability, activity, and tolerability of ADCs.[22−25] Attempts to replace the bisglucamine motif with other hydrophilic groups led to higher levels of aggregation. However, incorporating the more hydrophilic payload **15** resulted in improved anti-tumor activity (Figure 6) for ADC **42** compared to the HT-19 version of **37** while having no additional effects on body weight (see Figure S3 in the Supporting Information).

The more hydrophilic payload **15** also impacted the necessity of the large solubilizing motif in the scaffold. In fact, lower-molecular-weight scaffolds (Figure 7A) were identified through replacement of the PEG8-bisglucamine scaffold with a carboxylic acid, which maintained a similar hydrophilicity profile (Figure 7B). Attempts to optimize the carboxylic acid location and the stereochemistry led to the dipeptides **43**−**46**, which exemplify the significant impact a subtle design component can have on the in vivo performance of the ADC. The four ADCs share the same payload, antibody, linker-type, and conjugation type and only vary in the stereochemistry of the glutamic acid (solubility group) and the alanine adjacent to the linker. Interestingly, the level of in vivo activity, which was assessed in the SKOV3 xenograft model, varied greatly (Figure 7C). All of the ADCs showed some level of anti-tumor activity after a single 1 mg/kg dose administration; however, the (D)-alanine was detrimental to the ADC's activity. The stereochemistry at the glutamic acid had some effect on the ADC's activity, but less so compared to the effect of the alanine's stereochemistry.

The optimal low-MW scaffolds appeared to have comparable activity to that of the PEG8-bisglucamine scaffold and synthetically were more amenable from a development standpoint. However, before deciding to prioritize a low-MW scaffold for the STING agonist ADC platform, a more complete, head-to-head characterization was conducted. As such, the PEG8-bisglucamine scaffold (exemplified by **42**) and the optimal low-MW scaffold (exemplified by **43**) were coupled with lead payload **19b** (resulting in ADCs **47** and **48**, respectively) and characterized in vitro and in vivo to select the lead platform. Analytical (see Figure S4 in the Supporting Information) and in vitro characterization using co-cultures of antigen-expressing cancer cells and reporter THP1 monocytic immune cells or PBMCs (Figure 8A) showed the ADCs to be comparable and non-differentiated. In vivo characterization showed similar anti-tumor activity (Figure 8B), but consistently higher exposure was observed with PEG8-bisglucamine ADC **47** compared to the low-MW scaffold ADC **48**. For example, in a mouse PK study (Figure 8C), the conjugated drug (parameter measuring drug conjugated to the antibody representative of ADC exposure) of **48** was cleared more quickly than **47**. Similar results were observed in non-human primates (Figure 8D), which resulted in greater levels of free drug being measured after administration of **48**. Additionally, administration of **48** at 9 mg/kg led to elevated levels of white blood cells and neutrophils (Figure 8E) in non-human primates. Although these hematologic changes were not associated with any clinical signs, this observation and the faster clearance rates led to the deprioritization of the low-MW scaffolds. Satisfyingly, ADC **47** was shown to have a consistent PK profile across species, being highly stable with minimal free drug being observed, and showed minimal to no effects on hematology parameters in non-human primates at the same dose level of 9 mg/kg. Based on the anti-tumor activity, PK, and tolerability profile, the PEG8-bisglucamine scaffold with lead payload **19b** was chosen as the lead platform (also known as Immunosynthen), and ADC **47** (also known as XMT-2056) was selected for further development. Further preclinical characterization of XMT-2056 has been reported elsewhere.[14]

CONCLUSIONS

STING agonists have demonstrated robust preclinical anti-tumor activity and have the potential to be a transformative immuno-oncology treatment. Unfortunately, translation of this potential to the clinic has been limited, with reports of intratumorally administered STING agonists having modest clinical benefit. A STING agonist ADC could overcome many of the potential limitations of intratumorally administered or non-targeted systemically administered STING agonists through localization of the STING agonist in the tumor microenvironment, resulting in greater anti-tumor activity and improved tolerability.

Here, we have described the development of a STING agonist ADC platform through a rigorous and data-driven approach. Optimization of the STING agonist was performed with specific considerations for an ADC, including activity and PK parameters such as cell permeability and stability. Structure-based medicinal chemistry efforts allowed for modification within the payload's core scaffold to improve the hydrophilic nature, leading to the lead payload selection. Head-to-head evaluation of cleavable and non-cleavable linkers in in vivo studies identified an ester cleavable linker as the best fit for a STING agonist platform. Incorporation of a hydrophilic scaffold resulted in identification of the lead platform based on the resulting ADC's anti-tumor activity, PK profile across non-clinical species, and tolerability as assessed in non-human primates. Conjugation of the lead STING agonist platform to a HER2-targeted antibody (drug-to-antibody ratio = 8) resulted in the development of XMT-2056,[14] which is currently under further investigation.

EXPERIMENTAL SECTION

General Procedures. Nuclear magnetic resonance (NMR) spectra were recorded on either a Bruker 400 MHz or a 500 mHz NMR spectrometer. The data were processed with MestReNova software. LCMS data were collected with a Waters Acquity UPLC I-Class system (Agilent InfinityLab Poroshell 120 EC-C18) with a Bruker Compact quadruple time-of-flight spectrometer (ESI-TOF positive mode). A 95:5 A/B to 5:95 A/B gradient was used with the mobile A phase being water with 0.1% formic acid and the B phase being acetonitrile with 0.1% formic acid. All purified compounds possessed >95% purity based on HPLC assessment. ADC characterization was assessed by SEC, HIC, and UV−vis and described in detail in the Materials section focused on ADC synthesis.

Materials. Synthesis of compounds **4**−**17** was completed similar to previously published synthetic routes.[6]

(E)-7-(3-Aminopropoxy)-1-(4-(5-carbamoyl-2-(1-ethyl-3-methyl-1H-pyrazole-5-carboxamido)-7-methoxy-1H-benzo[d]imidazole-1-

https://doi.org/10.1021/acs.jmedchem.3c00907
J. Med. Chem. 2023, 66, 10715−10733

yl)but-2-en-1-yl)-2-(1-ethyl-3-methyl-1H-pyrazole-5-carboxamido)-1H-benzo[d]imidazole-5-carboxamide, Compound ***4***. ^{1}H NMR (400 MHz, DMSO-d_6): δ 12.82 (br s, 1H), 8.00−7.94 (m, 5H), 7.66−7.64 (m, 2H), 7.37−7.32 (m, 4H), 6.52−6.49 (m, 2H), 5.82−5.78 (m, 2H), 4.95−4.88 (4H), 4.55−4.46 (m, 4H), 4.25−4.05 (m, 2H), 3.77−3.72 (m, 3H), 2.93−2.85 (m, 2H), 2.17−2.08 (m, 6H), 1.96−1.88 (m, 2H), 1.31−1.23 (m, 6H). ESI-MS: $C_{38}H_{46}N_{13}O_6$ (M + H), calcd 780.37; found, 780.35.

(E)-4-((5-Carbamoyl-1-(4-(5-carbamoyl-2-(1-ethyl-3-methyl-1H-pyrazole-5-carboxamido)-7-methoxy-1H-benzo[d]imidazole-1-yl)-but-2-en-1-yl)-2-(1-ethyl-3-methyl-1H-pyrazole-5-carboxamido)-1H-benzo[d]imidazole-7-yl)oxy)butanoic Acid, Compound ***5***. ^{1}H NMR (400 MHz, DMSO-d_6): δ 12.82 (br s, 1H), 7.96 (s, 2H), 7.64 (s, 2H), 7.34 (s, 2H), 7.31 (s, 2H), 6.50 (s, 2H), 5.89−5.76 (m, 2H), 4.95−4.87 (m, 4H), 4.55−4.47 (m, 6H), 4.05−3.97 (m, 3H), 3.74 (s, 3H), 2.33−2.26 (m, 2H), 2.10 (s, 6H), 1.88−1.80 (m, 2H), 1.25 (t, J = 7.2 Hz, 6H). ESI-MS: $C_{39}H_{45}N_{12}O_8$ (M + H), calcd 809.35; found, 809.34.

(E)-1-(4-(5-Carbamoyl-2-(1-ethyl-3-methyl-1H-pyrazole-5-carboxamido)-7-(3-hydroxypropoxy)-1H-benzo[d]imidazole-1-yl)but-2-en-1-yl)-2-(1-ethyl-3-methyl-1H-pyrazole-5-carboxamido)-7-methoxy-1H-benzo[d]imidazole-5-carboxamide, Compound ***6***. ^{1}H NMR (400 MHz, DMSO-d_6): δ 12.81 (s, 1H), 7.97 (s, 2H), 7.62 (d, J = 3.2 Hz, 2H), 7.34 (d, J = 10.4 Hz, 2H), 7.30 (s, 2H), 6.50 (s, 2H), 5.82 (s, 2H), 4.90 (s, 4H), 4.55−4.48 (m, 5H), 4.04 (t, J = 6.2 Hz, 2H), 3.73 (s, 3H), 3.46−3.40 (m, 3H), 2.10−2.06 (m, 6), 1.74−1.66 (m, 2H), 1.28−1.22 (m, 6H). ESI-MS: $C_{38}H_{45}N_{12}O_7$ (M + H), calcd 781.4; found, 781.3.

(E)-1-(4-(5-Carbamoyl-2-(1,2-dimethyl-1H-imidazole-5-carboxamido)-7-(3-hydroxypropoxy)-1H-benzo[d]imidazole-1-yl)but-2-en-1-yl)-2-(1,2-dimethyl-1H-imidazole-5-carboxamido)-7-methoxy-1H-benzo[d]imidazole-5-carboxamide, Compound ***7***. ^{1}H NMR (400 MHz, DMSO-d_6): δ 7.89 (d, J = 12.0 Hz, 2H), 7.59 (dd, J = 7.0, 1.3 Hz, 2H), 7.29 (d, J = 6.2 Hz, 2H), 5.80 (s, 2H), 4.95 (s, 4H), 3.95 (d, J = 5.3 Hz, 6H), 3.47 (s, 2H), 1.70 (t, J = 6.3 Hz, 2H). ESI-MS: $C_{36}H_{41}N_{12}O_7$ (M + H), calcd 753.31; found, 753.15.

(E)-N-(5-Carbamoyl-1-(4-(5-carbamoyl-2-(2,5-dimethyloxazole-4-carboxamido)-7-(3-hydroxypropoxy)-1H-benzo[d]imidazole-1-yl)but-2-en-1-yl)-7-methoxy-1H-benzo[d]imidazole-2-yl)-2,5-dimethyloxazole-4-carboxamide, Compound ***8***. ^{1}H NMR (400 MHz, DMSO-d_6): δ 12.65 (d, J = 15.3 Hz, 1H), 7.92 (s, 2H), 7.59 (d, J = 4.6 Hz, 2H), 7.28 (d, J = 19.8 Hz, 4H), 5.79−5.57 (m, 2H), 4.85 (s, 4H), 4.04 (t, J = 6.4 Hz, 2H), 3.74 (s, 3H), 3.44 (t, J = 5.5 Hz, 2H), 2.61 (s, 2H), 2.42 (d, J = 5.1 Hz, 6H), 2.31 (d, J = 6.3 Hz, 6H). ESI-MS: $C_{36}H_{39}N_{10}O_9$ (M + H), calcd 755.28; found, 755.10.

(E)-1-(4-(5-Carbamoyl-2-(3-ethyl-1-methyl-1H-pyrazole-4-carboxamido)-7-(3-hydroxypropoxy)-1H-benzo[d]imidazole-1-yl)but-2-en-1-yl)-2-(3-ethyl-1-methyl-1H-pyrazole-4-carboxamido)-7-methoxy-1H-benzo[d]imidazole-5-carboxamide, Compound ***9***. ^{1}H NMR (400 MHz, DMSO-d_6): δ 7.92 (d, J = 15.8 Hz, 2H), 7.55 (d, J = 4.1 Hz, 2H), 7.23 (s, 2H), 5.78 (m, 2H), 4.86 (d, J = 7.2 Hz, 2H), 3.99 (s, 2H), 3.69 (d, J = 14.7 Hz, 6H), 2.81 (s, 4H), 1.66 (s, 2H), 1.11−1.05 (m, 6H). ESI-MS: $C_{38}H_{45}N_{12}O_7$ (M + H), calcd 781.35; found, 781.20.

(E)-1-(4-(5-Carbamoyl-2-(1-ethyl-3-methyl-1H-pyrazole-5-carboxamido)-7-methoxy-1H-benzo[d]imidazole-1-yl)but-2-en-1-yl)-2-(3-ethyl-1-methyl-1H-pyrazole-4-carboxamido)-7-(3-hydroxypropoxy)-1H-benzo[d]imidazole-5-carboxamide, Compound ***10***. ^{1}H NMR (400 MHz, methanol-d_4): δ 7.89 (s, 1H), 7.52 (d, J = 16.5 Hz, 2H), 7.31−7.22 (m, 2H), 6.54 (s, 1H), 5.81 (d, J = 3.3 Hz, 2H), 4.99 (d, J = 7.0 Hz, 4H), 4.58 (s, 3H), 4.01 (d, J = 6.5 Hz, 2H), 3.77 (s, 3H), 3.74 (s, 2H), 3.59 (t, J = 6.2 Hz, 2H), 2.90 (d, J = 7.7 Hz, 2H), 2.16 (s, 3H), 1.84−1.74 (m, 2H), 1.27 (d, J = 6.7 Hz, 3H), 1.16 (d, J = 7.5 Hz, 3H). ESI-MS: $C_{38}H_{45}N_{12}O_7$ (M + H), calcd 781.35; found, 781.20.

(E)-N-(5-Carbamoyl-1-(4-(5-carbamoyl-2-(4-ethyl-2-methylthiazole-5-carboxamido)-7-(3-hydroxypropoxy)-1H-benzo[d]-imidazole-1-yl)but-2-en-1-yl)-7-methoxy-1H-benzo[d]imidazole-2-yl)-4-ethyl-2-methylthiazole-5-carboxamide, Compound ***11***. ^{1}H NMR (400 MHz, DMSO-d_6): δ 12.72 (s, 2H), 7.93 (s, 2H), 7.57 (dd, J = 3.6, 1.3 Hz, 2H), 7.36−7.23 (m, 4H), 5.90−5.83 (m, 2H), 4.83 (s, 4H), 4.05 (t, J = 6.4 Hz, 2H), 3.75 (s, 3H), 3.44 (d, J = 5.3 Hz, 2H), 3.09−3.04 (m, 4H), 2.61 (s, 6H), 1.72 (t, J = 6.3 Hz, 2H), 1.11 (dd, J = 7.5, 1.2 Hz, 6H). ESI-MS: $C_{38}H_{43}N_{10}O_7S_2$ (M + H), calcd 815.27; found, 815.20.

(E)-N-(5-Carbamoyl-1-(4-(5-carbamoyl-2-(1-ethyl-3-methyl-1H-pyrazole-5-carboxamido)-7-methoxy-1H-benzo[d]imidazole-1-yl)-but-2-en-1-yl)-7-(3-hydroxypropoxy)-1H-benzo[d]imidazole-2-yl)-4-ethyl-2-methylthiazole-5-carboxamide, Compound ***12***. ^{1}H NMR (400 MHz, methanol-d_4): δ 7.53 (dd, J = 4.8, 1.4 Hz, 2H), 7.31 (d, J = 1.4 Hz, 1H), 7.25 (d, J = 1.4 Hz, 1H), 6.53 (s, 1H), 5.93−5.77 (m, 2H), 4.99 (t, J = 6.2 Hz, 4H), 4.55 (q, J = 7.1 Hz, 2H), 4.14 (t, J = 6.2 Hz, 2H), 3.74 (s, 3H), 3.65 (t, J = 6.2 Hz, 2H), 3.15 (q, J = 7.6 Hz, 2H), 2.65 (s, 3H), 2.16 (s, 3H), 1.89 (p, J = 6.2 Hz, 2H), 1.31 (t, J = 7.1 Hz, 3H), 1.22 (t, J = 7.5 Hz, 3H). ESI-MS: $C_{38}H_{44}N_{11}O_7S$ (M + H), calcd 798.31; found, 798.30.

(E)-N-(5-Carbamoyl-1-(4-(5-carbamoyl-2-(1-ethyl-3-methyl-1H-pyrazole-5-carboxamido)-7-methoxy-1H-benzo[d]imidazole-1-yl)-but-2-en-1-yl)-7-(3-hydroxypropoxy)-1H-benzo[d]imidazole-2-yl)-4-ethyl-2-methyloxazole-5-carboxamide, Compound ***13***. ^{1}H NMR (400 MHz, methanol-d_4): δ 7.63−7.56 (m, 2H), 7.30 (s, 2H), 5.84 (d, J = 3.5 Hz, 2H), 5.03 (d, J = 3.7 Hz, 4H), 4.57 (q, J = 7.1 Hz, 2H), 4.09 (t, J = 6.2 Hz, 2H), 3.79 (s, 3H), 3.63 (t, J = 6.2 Hz, 2H), 2.87 (q, J = 7.6 Hz, 2H), 2.46 (s, 3H), 2.20 (s, 3H), 1.84 (p, J = 6.2 Hz, 2H), 1.33 (t, J = 7.1 Hz, 3H), 1.12 (t, J = 7.5 Hz, 3H). ESI-MS: $C_{38}H_{44}N_{11}O_8$ (M + H), calcd 782.33; found, 782.15.

(E)-N-(5-Carbamoyl-1-(4-(5-carbamoyl-2-(1-ethyl-3-methyl-1H-pyrazole-5-carboxamido)-7-(3-hydroxypropoxy)-1H-benzo[d]-imidazole-1-yl)but-2-en-1-yl)-7-methoxy-1H-benzo[d]imidazole-2-yl)-4-ethyl-2-methyloxazole-5-carboxamide, Compound ***14***. ^{1}H NMR (400 MHz, DMSO-d_6): δ 7.94 (s, 2H), 7.65−7.56 (m, 2H), 7.32−7.23 (m, 4H), 6.46 (s, 1H), 5.77 (d, J = 3.4 Hz, 2H), 4.86 (d, J = 16.8 Hz, 4H), 4.47 (d, J = 7.2 Hz, 2H), 4.02 (t, J = 6.4 Hz, 2H), 3.73 (s, 3H), 2.76 (t, J = 7.5 Hz, 2H), 2.61 (s, 2H), 2.07 (s, 3H), 1.66 (t, J = 6.2 Hz, 2H), 1.23 (d, J = 7.0 Hz, 3H), 0.96 (t, J = 7.5 Hz, 3H). ESI-MS: $C_{38}H_{44}N_{11}O_8$ (M + H), calcd 782.33; found, 782.30.

(E)-N-(5-Carbamoyl-1-(4-(5-carbamoyl-2-(4-ethyl-2-methyloxazole-5-carboxamido)-7-(3-hydroxypropoxy)-1H-benzo[d]-imidazole-1-yl)but-2-en-1-yl)-7-methoxy-1H-benzo[d]imidazole-2-yl)-4-ethyl-2-methyloxazole-5-carboxamide, Compound ***15***. ^{1}H NMR (400 MHz, DMSO-d_6): δ 12.67 (s, 2H), 7.92 (s, 2H), 7.59 (d, J = 4.6 Hz, 2H), 7.29 (d, J = 12.8 Hz, 4H), 5.75 (q, J = 4.7 Hz, 2H), 4.91−4.80 (m, 4H), 4.03 (t, J = 6.4 Hz, 2H), 3.73 (s, 3H), 3.43 (t, J = 5.8 Hz, 2H), 2.75 (dt, J = 12.6, 6.4 Hz, 4H), 2.35 (d, J = 2.2 Hz, 6H), 1.69 (t, J = 6.3 Hz, 2H), 0.96 (q, J = 7.5 Hz, 6H). ESI-MS: $C_{38}H_{43}N_{10}O_9$ (M + H), calcd 783.31; found, 783.30.

Compound ***16***. ESI-MS: $C_{34}H_{35}N_{10}O_9$ (M + H), calcd 727.26; found, 727.21.

Compound ***17***. ESI-MS: $C_{36}H_{39}N_{10}O_9$ (M + H), calcd 755.29; found, 755.23.

Synthesis and Characterization of Compounds 18a−e. *tert-Butyl (E)-(4-((4-carbamoyl-2-methoxyphenyl)amino)but-2-en-1-yl)carbamate, Compound* ***21***. To a stirred solution of 4-amino-3-methoxybenzamide, compound **20** (7.0 g, 42.2 mmol), in DMF (35 mL), were added *tert*-butyl (*E*)-(4-bromobut-2-en-1-yl)carbamate (12.6 g, 50.6 mmol) and K_2CO_3 (8.74 g, 63.3 mmol). The mixture was heated to 100 °C and stirred for 16 h, and then, it was diluted in water and extracted with EtOAc (3×). The combined organic layers were dried over Na_2SO_4 and concentrated in vacuo. Purification over silica gel (DCM/MeOH 10:1 v/v) afforded *tert*-butyl (*E*)-(4-((4-carbamoyl-2-methoxyphenyl)amino)but-2-en-1-yl)carbamate, compound **21** (6.0 g, 42% yield), as a white solid. ^{1}H NMR (400 MHz, DMSO-d_6): δ 7.61 (s, 1H), 7.37 (dd, J = 8.2, 1.9 Hz, 1H), 7.32 (d, J = 1.9 Hz, 1H), 6.99−6.87 (m, 2H), 6.45 (d, J = 8.3 Hz, 1H), 5.60−5.45 (m, 3H), 3.81 (s, 3H), 3.74 (d, J = 6.0 Hz, 2H), 3.56−3.45 (m, 2H), 1.36 (s, 9H). ESI-MS: $C_{17}H_{26}N_3O_4$ (M + H), calcd 336.18; found, 336.20.

tert-Butyl (E)-(4-(6-carbamoyl-2-imino-4-methoxybenzo[d]-thiazol-3(2H)-yl)but-2-en-1-yl)carbamate, Compound ***22***. To a stirred solution of *tert*-butyl (*E*)-(4-((4-carbamoyl-2-methoxyphenyl)-amino)but-2-en-1-yl)carbamate, compound **21** (6.7 g, 20.0 mmol), in acetic acid (12 mL), was added KSCN (7.77 g, 80.0 mmol), and the mixture was stirred at room temperature for 30 min. Then, Br_2 (1 mL,

https://doi.org/10.1021/acs.jmedchem.3c00907
J. Med. Chem. 2023, 66, 10715−10733

20.0 mmol) dissolved in acetic acid (8 mL) was added dropwise, and the resulting mixture was stirred at room temperature for 16 h. The mixture was quenched with water and the solids were filtered. The filtrate was adjusted to pH 9 with aqueous ammonia and extracted with EtOAc (3×). The combined organic layers were dried over Na_2SO_4 and concentrated in vacuo to afford *tert*-butyl (*E*)-(4-(6-carbamoyl-2-imino-4-methoxybenzo[*d*]thiazol-3(2*H*)-yl)but-2-en-1-yl)carbamate, compound **22** (5.0 g, 63% yield), as a brown solid. ^{1}H NMR (400 MHz, DMSO-d_6): δ 8.41 (s, 1H), 7.87 (s, 1H), 7.53 (d, J = 1.6 Hz, 1H), 7.44−7.37 (m, 1H), 7.30 (d, J = 12.6 Hz, 1H), 6.95 (t, J = 5.9 Hz, 1H), 5.67−5.47 (m, 2H), 4.77 (d, J = 5.3 Hz, 2H), 3.86 (s, 3H), 3.48 (t, J = 5.3 Hz, 2H), 1.35 (d, J = 7.5 Hz, 9H). ESI-MS: $C_{18}H_{25}N_4O_4S$ (M + H), calcd 393.15; found, 393.50.

tert-Butyl ((E)-4-((Z)-6-carbamoyl-2-((4-ethyl-2-methyloxazole-5-carbonyl)imino)-4-methoxybenzo[d]thiazol-3(2H)-yl)but-2-en-1-yl)carbamate, Compound ***23b****.* To a stirred solution of *tert*-butyl (*E*)-(4-(6-carbamoyl-2-imino-4-methoxybenzo[*d*]thiazol-3(2*H*)-yl)-but-2-en-1-yl)carbamate, compound **22** (2.0 g, 5.10 mmol), in DMF (20 mL), were added 4-ethyl-2-methyloxazole-5-carboxylic acid (948 mg, 6.12 mmol), HATU (2.91 g, 7.65 mmol), and DIPEA (4.44 mL, 25.50 mmol). The mixture was stirred for 16 h and then quenched with water. The resulting solid was filtered and washed with water to afford *tert*-butyl ((*E*)-4-((Z)-6-carbamoyl-2-((4-ethyl-2-methyloxazole-5-carbonyl)imino)-4-methoxybenzo[*d*]thiazol-3(2*H*)-yl)but-2-en-1-yl)carbamate, compound **23b** (2.0 g, 74% yield), as a white solid. ^{1}H NMR (400 MHz, DMSO-d_6): δ 8.08 (s, 1H), 7.97 (d, J = 14.0 Hz, 1H), 7.61 (s, 1H), 7.49 (s, 1H), 6.92 (t, J = 5.9 Hz, 1H), 5.81−5.60 (m, 2H), 5.31 (d, J = 5.7 Hz, 2H), 3.99 (s, 3H), 3.51 (d, J = 5.7 Hz, 2H), 2.99 (q, J = 7.6 Hz, 2H), 2.47 (s, 3H), 1.31 (s, 9H), 1.05−0.95 (m, 3H). ESI-MS: $C_{25}H_{32}N_5O_6S$ (M + H), calcd 530.20; found, 530.30.

N-((Z)-3-((E)-4-Aminobut-2-en-1-yl)-6-carbamoyl-4-methoxybenzo[d]thiazol-2(3H)-ylidene)-4-ethyl-2-methyloxazole-5-carboxamide, Compound ***28b****.* *tert*-Butyl ((*E*)-4-((*Z*)-6-carbamoyl-2-((4-ethyl-2-methyloxazole-5-carbonyl)imino)-4-methoxybenzo-[*d*]thiazol-3(2*H*)-yl)but-2-en-1-yl)carbamate, compound **23b** (2.0 g, 3.78 mmol), was stirred in HCl (4 M in dioxane, 100 mL) for 6 h. The mixture was concentrated in vacuo to afford *N*-((*Z*)-3-((*E*)-4-aminobut-2-en-1-yl)-6-carbamoyl-4-methoxybenzo[*d*]thiazol-2(3*H*)-ylidene)-4-ethyl-2-methyloxazole-5-carboxamide-HCl, compound **28b** (2.0 g, 100% yield), as a white solid. ^{1}H NMR (400 MHz, DMSO-d_6): δ 8.16 (s, 1H), 8.06 (s, 2H), 8.03 (d, J = 1.5 Hz, 1H), 7.66 (d, J = 1.5 Hz, 1H), 7.51 (s, 1H), 6.07 (dt, J = 15.7, 5.7 Hz, 1H), 5.69 (dt, J = 15.6, 6.3 Hz, 1H), 5.37 (d, J = 5.6 Hz, 2H), 3.98 (s, 3H), 3.42 (p, J = 6.0 Hz, 2H), 3.00 (q, J = 7.6 Hz, 2H), 2.48 (s, 3H), 1.22 (t, J = 7.5 Hz, 3H). ESI-MS: $C_{20}H_{24}N_5O_4S$ (M + H), calcd 430.15; found, 430.25.

N-((Z)-3-((E)-4-((2-(3-((tert-Butyldimethylsilyl)oxy)propoxy)-4-carbamoyl-6-nitrophenyl)amino)but-2-en-1-yl)-6-carbamoyl-4-methoxybenzo[d]thiazol-2(3H)-ylidene)-4-ethyl-2-methyloxazole-5-carboxamide, Compound ***30b****.* To a stirred solution of 3-(3-((*tert*-butyldimethylsilyl)oxy)propoxy)-4-chloro-5-nitrobenzamide (800 mg, 2.15 mmol) in DMSO (2.5 mL) were added *N*-((Z)-3-((*E*)-4-aminobut-2-en-1-yl)-6-carbamoyl-4-methoxybenzo[*d*]thiazol-2(3*H*)-ylidene)-4-ethyl-2-methyloxazole-5-carboxamide-HCl, compound **28b** (1.2 g, 2.58 mmol), and Et_3N (1.5 mL, 10.75 mmol). The mixture was stirred at room temperature for 5 h and then quenched with water. The resulting solid was filtered and washed with water to afford *N*-((*Z*)-3-((*E*)-4-((2-(3-((*tert*-butyldimethylsilyl)oxy)propoxy)-4-carbamoyl-6-nitrophenyl)amino)but-2-en-1-yl)-6-carbamoyl-4-methoxybenzo[*d*]thiazol-2(3*H*)-ylidene)-4-ethyl-2-methyloxazole-5-carboxamide, compound **30b** (800 mg, 47% yield), as a yellow solid. ^{1}H NMR (400 MHz, DMSO-d_6): δ 8.13−8.05 (m, 2H), 8.02−7.93 (m, 2H), 7.67 (t, J = 6.3 Hz, 1H), 7.57 (d, J = 1.5 Hz, 1H), 7.51−7.42 (m, 2H), 7.28 (s, 1H), 5.80 (dt, J = 15.7, 5.6 Hz, 1H), 5.67 (dt, J = 15.6, 5.6 Hz, 1H), 5.27 (d, J = 5.6 Hz, 2H), 4.12 (t, J = 5.9 Hz, 2H), 3.96 (t, J = 6.1 Hz, 2H), 3.89 (s, 3H), 3.61 (t, J = 6.2 Hz, 2H), 2.90 (q, J = 7.5 Hz, 2H), 1.78 (t, J = 6.1 Hz, 2H), 1.13 (t, J = 7.5 Hz, 3H), 0.78 (s, 9H), −0.07 (s, 6H). ESI-MS: $C_{36}H_{48}N_7O_9SSi$ (M + H), calcd 782.29; found, 782.30.

N-((Z)-3-((E)-4-((2-Amino-6-(3-((tert-butyldimethylsilyl)oxy)-propoxy)-4-carbamoylphenyl)amino)but-2-en-1-yl)-6-carbamoyl-4-methoxybenzo[d]thiazol-2(3H)-ylidene)-4-ethyl-2-methyloxazole-5-carboxamide, Compound ***32b****.* To a stirred solution of *N*-((*Z*)-3-((*E*)-4-((2-(3-((*tert*-butyldimethylsilyl)oxy)propoxy)-4-carbamoyl-6-nitrophenyl)amino)but-2-en-1-yl)-6-carbamoyl-4-methoxybenzo[*d*]thiazol-2(3*H*)-ylidene)-4-ethyl-2-methyloxazole-5-carboxamide, compound **30b** (1.30 g, 1.66 mmol), in MeOH (30 mL) at 0 °C, was added $Na_2S_2O_4$ (5.79 g, 33.28 mmol) dissolved in water (7.5 mL), followed immediately by aqueous NH_4OH (6.0 mL, 41.58 mmol). The mixture was allowed to warm to room temperature and stirred for 4 h and then it was diluted with water and extracted with EtOAc (2×). The combined organic layers were dried over Na_2SO_4 and concentrated in vacuo. Purification over silica gel (DCM/MeOH 9:1 v/v) afforded *N*-((*Z*)-3-((*E*)-4-((2-amino-6-(3-((*tert*-butyldimethylsilyl)oxy)propoxy)-4-carbamoylphenyl)amino)-but-2-en-1-yl)-6-carbamoyl-4-methoxybenzo[*d*]thiazol-2(3*H*)-ylidene)-4-ethyl-2-methyloxazole-5-carboxamide, compound **32b** (700 mg, 56% yield), as a yellow solid. ^{1}H NMR (400 MHz, DMSO-d_6): δ 8.07 (s, 1H), 7.98 (dd, J = 5.5, 1.5 Hz, 1H), 7.59 (d, J = 1.5 Hz, 2H), 7.51−7.42 (m, 1H), 6.96−6.91 (m, 1H), 6.81 (d, J = 1.8 Hz, 1H), 6.70 (d, J = 1.8 Hz, 1H), 5.87−5.67 (m, 2H), 5.29 (d, J = 5.6 Hz, 2H), 4.62 (s, 2H), 3.90 (s, 3H), 3.87 (q, J = 5.9, 4.4 Hz, 2H), 3.60 (t, J = 6.1 Hz, 2H), 2.97 (p, J = 7.7 Hz, 2H), 1.72 (p, J = 6.2 Hz, 2H), 1.17 (t, J = 7.5 Hz, 3H), 0.76 (d, J = 12.7 Hz, 9H), −0.08 (s, 6H). ESI-MS: $C_{36}H_{50}N_7O_7SSi$ (M + H), calcd 752.32; found, 752.15.

N-(5-Carbamoyl-1-((E)-4-((Z)-6-carbamoyl-2-((4-ethyl-2-methyloxazole-5-carbonyl)imino)-4-methoxybenzo[d]thiazol-3(2H)-yl)-but-2-en-1-yl)-7-(3-hydroxypropoxy)-1H-benzo[d]imidazole-2-yl)-4-ethyl-2-methyloxazole-5-carboxamide, Compound ***18b****.* To a stirred solution of *N*-((*Z*)-3-((*E*)-4-((2-amino-6-(3-((*tert*-butyldimethylsilyl)oxy)propoxy)-4-carbamoylphenyl)amino)but-2-en-1-yl)-6-carbamoyl-4-methoxybenzo[*d*]thiazol-2(3*H*)-ylidene)-4-ethyl-2-methyloxazole-5-carboxamide, compound **32b** (70 mg, 0.09 mmol), in methanol (5 mL), was added cyanogen bromide (19 mg, 0.19 mmol). The mixture was stirred at room temperature for 16 h and then concentrated in vacuo. The residue was triturated in pentane and filtered to afford *N*-((*Z*)-3-((*E*)-4-(2-amino-7-(3-((*tert*-butyldimethylsilyl)oxy)propoxy)-5-carbamoyl-1*H*-benzo[*d*]imidazole-1-yl)but-2-en-1-yl)-6-carbamoyl-4-methoxybenzo[*d*]thiazol-2(3*H*)-ylidene)-4-ethyl-2-methyloxazole-5-carboxamide (70 mg, 88% yield) as a gray solid. ^{1}H NMR (400 MHz, DMSO-d_6): δ 8.46 (s, 2H), 8.05 (d, J = 12.4 Hz, 2H), 8.00−7.95 (m, 1H), 7.57 (s, 1H), 7.46 (t, J = 19.2 Hz, 3H), 7.34 (s, 1H), 5.88 (dt, J = 15.8, 5.5 Hz, 1H), 5.78−5.69 (m, 1H), 5.29 (d, J = 5.4 Hz, 2H), 4.84 (d, J = 5.5 Hz, 2H), 4.05 (t, J = 6.2 Hz, 2H), 3.81 (s, 3H), 3.60 (t, J = 6.2 Hz, 2H), 2.80 (q, J = 7.5 Hz, 2H), 2.43 (s, 3H), 1.72 (p, J = 6.3 Hz, 2H), 1.04 (t, J = 7.5 Hz, 3H), 0.80 (s, 9H), −0.11 (s, 6H). ESI-MS: $C_{37}H_{49}N_8O_7SSi$ (M + H), calcd 777.31; found, 777.30.

To a stirred solution of *N*-((*Z*)-3-((*E*)-4-(2-amino-7-(3-((*tert*-butyldimethylsilyl)oxy)propoxy)-5-carbamoyl-1*H*-benzo[*d*]imidazole-1-yl)but-2-en-1-yl)-6-carbamoyl-4-methoxybenzo[*d*]thiazol-2(3*H*)-ylidene)-4-ethyl-2-methyloxazole-5-carboxamide (220 mg, 0.26 mmol) in DMF (2 mL) were added 4-ethyl-2-methyloxazole-5-carboxylic acid (59 mg, 0.38 mmol), PyBOP (199 mg, 0.38 mmol), and DIPEA (0.22 mL, 1.28 mmol). The mixture was stirred at 125 °C for 16 h and then it was concentrated in vacuo. The resulting residue was triturated in cold water and filtered. The solid was purified by HPLC (ACN/H_2O) to afford *N*-(5-carbamoyl-1-((*E*)-4-((*Z*)-6-carbamoyl-2-((4-ethyl-2-methyloxazole-5-carbonyl)imino)-4-methoxybenzo[*d*]thiazol-3(2*H*)-yl)but-2-en-1-yl)-7-(3-hydroxypropoxy)-1*H*-benzo[*d*]imidazole-2-yl)-4-ethyl-2-methyloxazole-5-carboxamide, compound **18b** (130 mg, 63%), as a white solid. ^{1}H NMR (400 MHz, DMSO-d_6): δ 8.05 (s, 1H), 7.97 (s, 2H), 7.62 (s, 1H), 7.54 (s, 1H), 7.49 (s, 1H), 7.31 (s, 2H), 5.82 (d, J = 4.0 Hz, 2H), 5.28 (s, 2H), 4.90 (s, 2H), 4.06 (t, J = 6.3 Hz, 2H), 3.80 (s, 3H), 3.45 (q, J = 5.8 Hz, 2H), 2.85−2.73 (m, 4H), 1.71 (t, J = 6.3 Hz, 2H), 1.00 (t, J = 7.5 Hz, 6H). ESI-MS: $C_{38}H_{42}N_9O_9S$ (M + H), calcd 800.27; found, 800.20.

https://doi.org/10.1021/acs.jmedchem.3c00907
J. Med. Chem. 2023, 66, 10715−10733

(Z)-3-((E)-4-(5-Carbamoyl-2-(1-ethyl-3-methyl-1H-pyrazole-5-carboxamido)-7-(3-hydroxypropoxy)-1H-benzo[d]imidazole-1-yl)-but-2-en-1-yl)-2-((1-ethyl-3-methyl-1H-pyrazole-5-carbonyl)-imino)-4-methoxy-2,3-dihydrobenzo[d]thiazole-6-carboxamide, Compound ***18a.*** ^{1}H NMR (400 MHz, DMSO-d_6): δ 8.08 (s, 1H), 7.98 (d, J = 1.5 Hz, 2H), 7.66−7.47 (m, 3H), 7.38−7.27 (m, 2H), 6.62 (s, 1H), 6.49 (s, 1H), 5.87 (q, J = 4.5 Hz, 2H), 5.31 (s, 2H), 4.93 (s, 2H), 4.59−4.50 (m, 4H), 4.04 (t, J = 6.4 Hz, 2H), 3.77 (s, 3H), 3.46−3.41 (m, 2H), 2.09 (d, J = 3.7 Hz, 6H), 1.67 (t, J = 6.2 Hz, 2H), 1.27 (dt, J = 7.1, 3.5 Hz, 6H). ESI-MS: $C_{38}H_{44}N_{11}O_7S$ (M + H), calcd 798.31; found, 798.20.

N-(5-Carbamoyl-1-((E)-4-((Z)-6-carbamoyl-2-((1-ethyl-3-methyl-1H-pyrazole-5-carbonyl)imino)-4-methoxybenzo[d]thiazol-3(2H)-yl)but-2-en-1-yl)-7-(3-hydroxypropoxy)-1H-benzo[d]imidazole-2-yl)-4-ethyl-2-methyloxazole-5-carboxamide, Compound ***18c.*** ^{1}H NMR (400 MHz, DMSO-d_6): δ 8.04 (s, 1H), 7.94 (d, J = 1.5 Hz, 2H), 7.59 (d, J = 1.3 Hz, 1H), 7.50 (d, J = 1.5 Hz, 1H), 7.46 (s, 1H), 7.31−7.26 (m, 2H), 6.56 (s, 1H), 5.91−5.74 (m, 2H), 5.27 (d, J = 4.4 Hz, 2H), 4.87 (s, 2H), 4.47 (t, J = 7.1 Hz, 2H), 4.02 (d, J = 6.3 Hz, 2H), 3.75 (s, 3H), 3.41 (d, J = 6.0 Hz, 2H), 2.76 (q, J = 7.5 Hz, 2H), 2.35 (s, 3H), 2.07 (s, 3H), 1.67 (t, J = 6.2 Hz, 2H), 1.24 (t, J = 7.1 Hz, 3H), 0.96 (t, J = 7.6 Hz, 3H). ESI-MS: $C_{38}H_{43}N_{10}O_8S$ (M + H), calcd 799.29; found, 799.30.

N-(5-Carbamoyl-1-((E)-4-((Z)-6-carbamoyl-2-((1-ethyl-3-methyl-1H-pyrazole-5-carbonyl)imino)-4-methoxybenzo[d]thiazol-3(2H)-yl)but-2-en-1-yl)-7-(3-hydroxypropoxy)-1H-benzo[d]imidazole-2-yl)-2,4-dimethyloxazole-5-carboxamide, Compound ***18d.*** ^{1}H NMR (400 MHz, DMSO-d_6): δ 8.04 (s, 1H), 7.94 (d, J = 1.6 Hz, 2H), 7.60 (d, J = 1.2 Hz, 1H), 7.50 (d, J = 1.6 Hz, 1H), 7.46 (s, 1H), 7.28 (d, J = 4.5 Hz, 2H), 6.57 (s, 1H), 5.90−5.75 (m, 2H), 5.27 (d, J = 4.5 Hz, 2H), 4.88 (s, 2H), 4.47 (t, J = 7.0 Hz, 2H), 4.02 (s, 2H), 3.40 (t, J = 6.1 Hz, 2H), 2.34 (s, 3H), 2.25 (s, 3H), 2.07 (s, 3H), 1.71−1.61 (m, 2H), 1.24 (t, J = 7.1 Hz, 3H). ESI-MS: $C_{37}H_{41}N_{10}O_8S$ (M + H), calcd 785.28; found, 785.20.

N-(5-Carbamoyl-1-((E)-4-((Z)-6-carbamoyl-2-((4-ethyloxazole-5-carbonyl)-imino)-4-methoxybenzo[d]thiazol-3(2H)-yl)but-2-en-1-yl)-7-(3-hydroxypropoxy)-1H-benzo-[d]imidazole-2-yl)-4-ethyloxazole-5-carboxamide, Compound ***18e.*** ^{1}H NMR (400 MHz, DMSO-d_6): δ 8.38 (s, 1H), 8.26 (s, 1H), 8.06 (s, 1H), 7.99 (s, 2H), 7.59 (d, J = 31.1 Hz, 2H), 7.32 (s, 2H), 6.53 (s, 1H), 5.82 (d, J = 3.0 Hz, 2H), 5.31 (s, 2H), 4.92 (s, 2H), 4.06 (t, J = 6.5 Hz, 2H), 3.79 (s, 3H), 3.43 (d, J = 5.7 Hz, 2H), 2.85 (dt, J = 10.0, 5.0 Hz, 4H), 1.69 (t, J = 6.2 Hz, 2H), 1.02 (t, J = 7.5 Hz, 6H). ESI-MS: $C_{36}H_{38}N_9O_9S$ (M + H), calcd 772.24; found, 772.20.

General Synthetic Details for the Synthesis of 19a−d. To a stirred solution of 6-chloro-5-nitronicotinic acid (20 g, 98.7 mmol) in DMSO (250 mL), *tert*-butyl (*E*)-(4-aminobut-2-en-1-yl)carbamate hydrochloride (24.1 g, 108.6 mmol) and potassium carbonate (40.9 g, 296 mmol) were added. The reaction was stirred at room temperature for 16 h. Once complete, the reaction was poured into cold water (1.5 L) and acidified (pH 5−6) with 1 N HCl solution. The resulting solid was collected, washed with water, and dried under reduced pressure to afford compound **25** (30 g, 86%) as a yellow solid. ^{1}H NMR (400 MHz, DMSO-d_6): δ 8.96 (s,1H), 8.88 (s, 1H), 8.73 (s, 1H), 6.94 (s, 1H), 5.75−5.5 (m, 2H), 4.23 (t, J = 4.8 Hz, 2H), 3.52 (s, 2H), 2.54 (s, 1H), 1.35 (s, 9H) ESI-MS: $C_{15}H_{21}N_4O_6$ (M + H), calcd 353.14; found, 353.05.

HATU (64.8 g, 170.4 mmol) and DIPEA (74 mL, 426 mmol) were added to a solution of compound **25** (30 g, 85.2 mmol) in DMF (300 mL). After stirring for 10 min, ammonium chloride (22.8 g, 426 mmol) was added, and the mixture was stirred for 16 h at room temperature. The reaction mixture was poured onto ice cold water (2 L) and stirred for 1 h during which time, a solid had precipitated. The solid was collected and dried under reduced pressure to afford *tert*-butyl (*E*)-(4-((5-carbamoyl-3-nitropyridin-2-yl)amino)but-2-en-1-yl)-carbamate (24 g, 80% yield) as a yellow solid compound. ^{1}H NMR (400 MHz, DMSO-d_6): δ 9.00−8.82 (m, 3H), 8.10 (s, 1H), 7.47 (s, 1H), 6.96 (t, J = 5.6 Hz, 1H), 5.75−5.5 (m, 2H), 4.21 (t, J = 4.4 Hz, 2H), 3.51 (s, 2H), 1.35 (s, 9H); ESI-MS: $C_{15}H_{22}N_5O_5$ (M + H), calcd 352.15; found, 352.10.

A solution of sodium dithionite (5 equiv) in methanol (1.4 M) was added to *tert*-butyl (*E*)-(4-((5-carbamoyl-3-nitropyridin-2-yl)amino)-but-2-en-1-yl)carbamate (1 equiv) in water (0.5 M) at 0 °C. Ammonium hydroxide (15 equiv) was added and then the reaction was allowed to stir at room temperature for 10 min. The reaction mixture was diluted with water and extracted with ethyl acetate. The combined organic extracts were washed with brine, dried over sodium sulfate, filtered, and concentrated under reduced pressure to afford compound **26**, which was used without purification. ^{1}H NMR (400 MHz, DMSO-d_6): δ 7.94 (s, 1H), 7.53 (s, 1H), 7.10 (s, 1H), 6.96 (t, J = 5.2 Hz, 1H), 6.88 (s, 1H), 6.17 (t, J = 5.2 Hz, 1H), 5.70−5.50 (m, 2H), 4.82 (s, 2H), 3.99 (t, J = 4.8 Hz, 2H), 3.51 (s, 2H), 1.35 (s, 9H); ESI-MS: $C_{15}H_{24}N_5O_3$ (M + H), calcd 322.2; found, 322.2.

Compound **26** (1 equiv) was dissolved in DMF (0.2 M) and cooled to 0 °C before ring A-CO-NCS (0.4 M solution in dioxane, 0.6 equiv) was added, and the reaction was stirred for 10 min before a second batch of ring A-CO-NCS (0.4 M solution in dioxane, 0.2 equiv) was added. After an additional 10 min, a third batch of ring A-CO-NCS (0.4 M solution in dioxane, 0.2 equiv) was added. After an additional 10 min, EDCI (2.5 equiv) and triethylamine (5 equiv) were added and the reaction stirred at room temperature for 18 h. The reaction mixture was concentrated and then diluted with water and stirred for 1 h. The solids were collected, washed with EtOAc, and dried under vacuum to give compound **27**.

Compound **27** (1 equiv) was dissolved in dioxane (100 mL) before HCl (4 M in dioxane, 20 equiv) was added (0.1 M final reaction concentration). The reaction was stirred at room temperature for 2 h or until the reaction was complete. The reaction mixture was concentrated to give compound **29**, which was used without further purification.

To a solution of 3-(3-((*tert*-butyldimethylsilyl)oxy)propoxy)-4-fluoro-5-nitrobenzamide (1 equiv) in DMSO (0.12 M) at 0 °C was added triethylamine (7 equiv) followed by compound **29** (1.2 equiv). The reaction was stirred at room temperature for 3 h or until the reaction was complete as judged by TLC. The reaction mixture was cooled before being slowly poured into ice cold water. The resulting mixture was stirred for 1 h at room temperature and then extracted with 10% MeOH in DCM. The combined extracts were dried over Na_2SO_4 and concentrated under reduced pressure to give compound **31**.

To a solution of compound **31** (10 g, 13.6 mmol) in methanol (0.07 M) at 0 °C, a solution of sodium dithionite (5 equiv) in water (0.7 M) was added followed by ammonia (25% aqueous solution, 25 equiv). The reaction was stirred at room temperature for 10 min. The reaction mixture was diluted with water and extracted with 10% MeOH in DCM. The combined extracts were dried over Na_2SO_4 and concentrated under reduced pressure to provide compound **33**.

Compound **33** (1 equiv) was dissolved in DMF (0.08 M) and cooled to 0 °C before ring B-CO-NCS (0.4 M solution in dioxane, 1 equiv) was added and the reaction was stirred for 10 min before a second batch of ring B-CO-NCS (0.4 M solution in dioxane, 0.4 equiv) was added. After an additional 10 min, a third batch of ring B-CO-NCS (0.4 M solution in dioxane, 0.4 equiv) was added. After an additional 10 min, EDCI (5 equiv) and triethylamine (10 equiv) were added and the reaction stirred at room temperature for 18 h. Once complete as judged by TLC, the reaction mixture was concentrated and then diluted with water and stirred for 1 h. The solids were collected, dried under vacuum, and used without further purification. The solids were dissolved in methanol (0.05 M) before HCl (4 M in dioxane, 10 equiv) was added. The reaction was stirred at room temperature for 2 h or until the reaction was complete. The reaction mixture was filtered and the solid was washed with MeOH and dried under vacuum to give compound **19**.

(E)-3-(4-(5-Carbamoyl-2-(1-ethyl-3-methyl-1H-pyrazole-5-carboxamido)-7-(3-hydroxypropoxy)-1H-benzo[d]imidazole-1-yl)but-2-en-1-yl)-2-(1-ethyl-3-methyl-1H-pyrazole-5-carboxamido)-3H-imidazo[4,5-b]pyridine-6-carboxamide, Compound ***19a.*** ^{1}H NMR (400 MHz, DMSO-d_6): δ 8.74−8.67 (m, 1H), 8.12 (s, 2H), 7.96 (s, 1H), 7.63 (s, 1H), 7.52 (s, 1H), 7.32 (d, J = 8.1 Hz, 2H), 6.52 (d, J = 12.9 Hz, 2H), 5.97−5.79 (m, 2H), 4.92 (d, J = 5.1 Hz, 2H), 4.78 (d, J

https://doi.org/10.1021/acs.jmedchem.3c00907
J. Med. Chem. 2023, 66, 10715−10733

= 5.2 Hz, 2H), 4.50 (h, *J* = 7.1 Hz, 4H), 4.11 (t, *J* = 6.4 Hz, 2H), 3.46 (d, *J* = 6.0 Hz, 2H), 2.10 (s, 6H), 1.75 (t, *J* = 6.2 Hz, 2H), 1.26 (td, *J* = 7.1, 2.2 Hz, 6H). ESI-MS: $C_{36}H_{42}N_{13}O_6$ (M + H), calcd 752.33; found, 752.30.

(E)-N-(5-Carbamoyl-1-(4-(6-carbamoyl-2-(4-ethyl-2-methyloxazole-5-carboxamido)-3H-imidazo[4,5-b]pyridin-3-yl)but-2-en-1-yl)-7-(3-hydroxypropoxy)-1H-benzo[d]imidazole-2-yl)-4-ethyl-2-methyloxazole-5-carboxamide, Compound ***19b***. ^{1}H NMR (400 MHz, DMSO-d_6): δ 8.69 (d, *J* = 1.9 Hz, 1H), 8.17−8.09 (m, 2H), 7.95 (s, 1H), 7.62 (s, 1H), 7.52 (s, 1H), 7.32 (s, 2H), 5.90−5.77 (m, 2H), 4.89 (d, *J* = 5.1 Hz, 2H), 4.75 (d, *J* = 5.0 Hz, 2H), 4.12 (t, *J* = 6.4 Hz, 2H), 2.79 (p, *J* = 7.5 Hz, 4H), 2.40 (d, *J* = 3.7 Hz, 6H), 1.75 (t, *J* = 6.2 Hz, 2H), 0.98 (td, *J* = 7.6, 3.0 Hz, 6H). ESI-MS: $C_{36}H_{40}N_{11}O_8$ (M + H), calcd 754.30; found, 754.25.

(E)-N-(5-Carbamoyl-1-(4-(6-carbamoyl-2-(1-ethyl-3-methyl-1H-pyrazole-5-carboxamido)-3H-imidazo[4,5-b]pyridin-3-yl)but-2-en-1-yl)-7-(3-hydroxypropoxy)-1H-benzo[d]imidazole-2-yl)-4-ethyl-2-methyloxazole-5-carboxamide, Compound ***19c***. ESI-MS: $C_{36}H_{41}N_{12}O_7$ (M + H), calcd 753.32; found, 753.34.

(E)-N-(5-Carbamoyl-1-(4-(6-carbamoyl-2-(1-ethyl-3-methyl-1H-pyrazole-5-carboxamido)-3H-imidazo[4,5-b]pyridin-3-yl)but-2-en-1-yl)-7-(3-hydroxypropoxy)-1H-benzo[d]imidazole-2-yl)-2,4-dimethyloxazole-5-carboxamide, Compound ***19d***. ESI-MS: $C_{35}H_{39}N_{12}O_7$ (M + H), calcd 739.31; found, 739.32.

Synthesis and Characterization of Compound 34. *Methyl (E)-5-Bromo-6-((4-((tert-butoxycarbonyl)amino)but-2-en-1-yl)-amino)nicotinate.* To a stirred solution of methyl 5-bromo-6-chloronicotinate (10 g, 39.92 mmol) in DMSO (150 mL) were added *tert*-butyl (*E*)-(4-aminobut-2-en-1-yl)carbamate (10.66 g, 47.86 mmol) and DIPEA (20.8 mL, 160.04 mmol) at 0 °C. The mixture was allowed to warm to room temperature and stirred for 48 h. The mixture was quenched with ice water and stirred for 10 min and then extracted with EtOAc. The combined organic layers were dried over Na_2SO_4 and concentrated in vacuo. The residue was purified over silica gel (hexane/EtOAc 70:30 v/v) to afford methyl (*E*)-5-bromo-6-((4-((*tert*-butoxycarbonyl)amino)but-2-en-1-yl)amino)nicotinate (6.0 g, 38% yield) as a yellow oil. ^{1}H NMR (400 MHz, DMSO-d_6): δ 8.56 (d, *J* = 2.0 Hz, 1H), 8.09 (d, *J* = 2.0 Hz, 1H), 7.32 (t, *J* = 5.9 Hz, 1H), 6.92 (s, 1H), 5.65−5.45 (m, 2H), 4.01 (d, *J* = 7.1 Hz, 2H), 3.78 (s, 3H), 3.49 (d, *J* = 5.8 Hz, 2H), 1.35 (s, 9H). ESI-MS: $C_{16}H_{23}BrN_3O_4$ (M + H), calcd 400.08; found, 400.10.

Methyl (E)-6-((4-((tert-Butoxycarbonyl)amino)but-2-en-1-yl)-amino)-5-((3-methoxy-3-oxopropyl)thio)nicotinate. To a stirred solution of methyl (*E*)-5-bromo-6-((4-((*tert*-butoxycarbonyl)amino)-but-2-en-1-yl)amino)nicotinate (3.2 g, 7.99 mmol), methyl 3-mercaptopropanoate (2.67 mL, 23.98 mmol) and DIPEA (2.79 mL) in dioxane (40 mL), was added xantphos (462 mg, 0.80 mmol) followed by tris(dibenzylideneacetone)dipalladium(0) $Pd_2(dba)_3$ (366 mg, 0.40 mmol). The mixture was heated to 110 °C and stirred for 16 h and then quenched with water and extracted with EtOAc. The combined organic layers were dried over Na_2SO_4 and concentrated in vacuo. The residue was purified over silica gel (hexane/EtOAc 1:1 v/v) to afford methyl (*E*)-6-((4-((*tert*-butoxycarbonyl)amino)but-2-en-1-yl)amino)-5-((3-methoxy-3-oxopropyl)thio)nicotinate (3.0 g, 85% yield) as an orange oil. ^{1}H NMR (400 MHz, DMSO-d_6): δ 8.51 (d, *J* = 2.2 Hz, 1H), 7.90 (d, *J* = 2.2 Hz, 1H), 7.28 (t, *J* = 5.9 Hz, 1H), 6.90 (t, *J* = 5.9 Hz, 1H), 5.63−5.40 (m, 2H), 4.05−3.96 (m, 2H), 3.74 (s, 3H), 3.53 (s, 3H), 3.46 (t, *J* = 5.7 Hz, 2H), 2.93 (t, *J* = 6.9 Hz, 2H), 2.53 (t, *J* = 6.9 Hz, 2H), 1.31 (s, 9H). ESI-MS: $C_{20}H_{30}N_3O_6S$ (M + H), calcd 440.18; found, 440.20.

Sodium (E)-2-((4-((tert-Butoxycarbonyl)amino)but-2-en-1-yl)-amino)-5-(methoxycarbonyl)pyridine-3-thiolate. To a stirred solution of methyl (*E*)-6-((4-((*tert*-butoxycarbonyl)amino)but-2-en-1-yl)amino)-5-((3-methoxy-3-oxopropyl)thio)nicotinate (3.0 g, 6.83 mmol) in THF (40 mL) was added NaOEt (21% in EtOH, 2.4 mL, 7.51 mmol), and the mixture was stirred at room temperature for 1 h. The mixture was diluted in DCM, and the resulting solid was filtered and washed with DCM to afford sodium (*E*)-2-((4-((*tert*-butoxycarbonyl)amino)but-2-en-1-yl)amino)-5-(methoxycarbonyl)-pyridine-3-thiolate (1.9 g, 74% yield) as a white solid. ^{1}H NMR (400 MHz, DMSO-d_6): δ 7.93 (d, *J* = 2.2 Hz, 1H), 7.54 (d, *J* = 2.2 Hz, 1H), 7.38 (t, *J* = 6.0 Hz, 1H), 6.98 (t, *J* = 5.8 Hz, 1H), 5.60 (qt, *J* = 15.5, 5.3 Hz, 2H), 4.01−3.93 (m, 2H), 3.53 (t, *J* = 5.8 Hz, 2H), 1.37 (s, 9H). ESI-MS: $C_{16}H_{22}N_3O_4S$ (M-H): 352.14; found, 352.10.

Methyl (E)-3-(4-((tert-Butoxycarbonyl)amino)but-2-en-1-yl)-2-imino-2,3-dihydrothiazolo[4,5-b]pyridine-6-carboxylate. To a stirred solution of sodium (*E*)-2-((4-((*tert*-butoxycarbonyl)amino)-but-2-en-1-yl)amino)-5-(methoxycarbonyl)pyridine-3-thiolate (1.9 g, 5.06 mmol) in MeOH (50 mL) at 0 °C was added BrCN (0.91 g, 8.60 mmol). The mixture was warmed to room temperature and stirred for 16 h. The resulting solid was filtered and washed with MeOH to afford methyl (*E*)-3-(4-((*tert*-butoxycarbonyl)amino)but-2-en-1-yl)-2-imino-2,3-dihydrothiazolo[4,5-*b*]pyridine-6-carboxylate (1.6 g, 84% yield) as a yellow solid. ^{1}H NMR (400 MHz, DMSO-d_6): δ 10.65 (s, 1H), 8.95−8.78 (m, 2H), 6.91 (q, *J* = 6.1 Hz, 1H), 5.72−5.53 (m, 2H), 4.83 (d, *J* = 5.3 Hz, 2H), 3.85 (d, *J* = 11.7 Hz, 3H), 3.52−3.42 (m, 2H), 1.29 (s, 9H). ESI-MS: $C_{17}H_{23}N_4O_4S$ (M + H), calcd 379.14; found, 379.10.

Methyl (Z)-3-((E)-4-((tert-Butoxycarbonyl)amino)but-2-en-1-yl)-2-((4-ethyl-2-methyloxazole-5-carbonyl)imino)-2,3-dihydrothiazolo[4,5-b]pyridine-6-carboxylate. To a stirred solution of methyl (*E*)-3-(4-((*tert*-butoxycarbonyl)amino)but-2-en-1-yl)-2-imino-2,3-dihydrothiazolo[4,5-*b*]pyridine-6-carboxylate (1.60 g, 4.23 mmol) and 4-ethyl-2-methyloxazole-5-carboxylic acid (0.98 g, 6.34 mmol) in DMF (20 mL) was added DIPEA (3.69 mL, 21.14 mmol) followed by HATU (3.21 g, 8.46 mmol). The mixture was stirred at room temperature for 6 h and then, it was diluted in water and stirred for 5 min. The resulting solid was filtered and dried to afford methyl (*Z*)-3-((*E*)-4-((*tert*-butoxycarbonyl)amino)but-2-en-1-yl)-2-((4-ethyl-2-methyloxazole-5-carbonyl)imino)-2,3-dihydrothiazolo[4,5-*b*]-pyridine-6-carboxylate (560 mg, 25% yield) as a white solid. ^{1}H NMR (400 MHz, DMSO-d_6): δ 9.01−8.79 (m, 2H), 6.89 (t, *J* = 6.0 Hz, 1H), 5.68 (qt, *J* = 16.1, 5.4 Hz, 2H), 5.01 (d, *J* = 5.5 Hz, 2H), 3.87 (s, 3H), 3.46 (t, *J* = 5.5 Hz, 2H), 3.31 (s, 3H), 2.98 (q, *J* = 7.5 Hz, 2H), 1.26 (s, 8H), 1.18 (t, *J* = 7.5 Hz, 3H). ESI-MS: $C_{24}H_{30}N_5O_6S$ (M + H), calcd 516.18; found, 516.20.

(Z)-3-((E)-4-((tert-Butoxycarbonyl)amino)but-2-en-1-yl)-2-((4-ethyl-2-methyloxazole-5-carbonyl)imino)-2,3-dihydrothiazolo[4,5-b]pyridine-6-carboxylic Acid. To a stirred solution of methyl (*Z*)-3-((*E*)-4-((*tert*-butoxycarbonyl)amino)but-2-en-1-yl)-2-((4-ethyl-2-methyloxazole-5-carbonyl)imino)-2,3-dihydrothiazolo[4,5-*b*]pyridine-6-carboxylate (560 mg, 1.09 mmol) in MeOH/THF/water (2:2:1 v/v/v, 50 mL) was added LiOH·H_2O (91 mg, 2.17 mmol). The mixture was stirred at room temperature for 4 h and then concentrated to remove the organic solvents. The residue was neutralized to pH < 7 with aqueous HCl, and the resulting solid was filtered and dried to afford (*Z*)-3-((*E*)-4-((*tert*-butoxycarbonyl)amino)but-2-en-1-yl)-2-((4-ethyl-2-methyloxazole-5-carbonyl)imino)-2,3-dihydrothiazolo-[4,5-*b*]pyridine-6-carboxylic acid (450 mg, 82% yield) as a white solid. ^{1}H NMR (400 MHz, DMSO-d_6): δ 8.99 (d, *J* = 1.9 Hz, 1H), 8.88 (d, *J* = 1.9 Hz, 1H), 6.92 (t, *J* = 5.9 Hz, 1H), 5.70 (pt, *J* = 19.9, 5.0 Hz, 2H), 5.06 (d, *J* = 5.5 Hz, 2H), 3.50 (t, *J* = 5.5 Hz, 2H), 3.03 (q, *J* = 7.5 Hz, 2H), 2.34 (s, 3H), 1.30 (s, 9H), 1.23 (t, *J* = 7.5 Hz, 3H). ESI-MS: $C_{23}H_{28}N_5O_6S$ (M + H), calcd 502.17; found, 502.20.

tert-Butyl ((E)-4-((Z)-6-Carbamoyl-2-((4-ethyl-2-methyloxazole-5-carbonyl)imino)thiazolo[4,5-b]pyridin-3(2H)-yl)but-2-en-1-yl)-carbamate. To a stirred solution of (*Z*)-3-((*E*)-4-((*tert*-butoxycarbonyl)amino)but-2-en-1-yl)-2-((4-ethyl-2-methyloxazole-5-carbonyl)imino)-2,3-dihydrothiazolo[4,5-*b*]pyridine-6-carboxylic acid (450 mg, 0.90 mmol) in DMF (10 mL) were added DIPEA (0.39 mL, 2.24 mmol), HATU (614 mg, 1.61 mmol), and NH_4Cl (145 mg, 2.69 mmol). The mixture was stirred at room temperature for 6 h and then diluted in water and stirred for 10 min. The resulting solid was filtered and dried to afford *tert*-butyl ((*E*)-4-((*Z*)-6-carbamoyl-2-((4-ethyl-2-methyloxazole-5-carbonyl)imino)thiazolo[4,5-*b*]pyridin-3(2*H*)-yl)-but-2-en-1-yl)carbamate (390 mg, 87% yield) as a white solid. ^{1}H NMR (400 MHz, DMSO-d_6): δ 8.92 (d, *J* = 2.0 Hz, 1H), 8.73 (d, *J* = 2.0 Hz, 1H), 8.16 (s, 1H), 7.62 (s, 1H), 6.89 (t, *J* = 5.8 Hz, 1H), 5.79−5.57 (m, 2H), 5.01 (d, *J* = 5.5 Hz, 2H), 3.46 (t, *J* = 5.3 Hz, 2H), 2.99 (q, *J* = 7.5 Hz, 2H), 2.45 (s, 3H), 1.26 (s, 9H), 1.19 (t, *J* = 7.5

https://doi.org/10.1021/acs.jmedchem.3c00907
J. Med. Chem. 2023, 66, 10715−10733

Hz, 3H). ESI-MS: $C_{23}H_{29}N_6O_5S$ (M + H), calcd 501.18; found, 501.20.

(E)-4-((Z)-6-Carbamoyl-2-((4-ethyl-2-methyloxazole-5-carbonyl)imino)thiazolo[4,5-b]pyridin-3(2H)-yl)but-2-en-1-aminium Chloride. A mixture of *tert*-butyl ((*E*)-4-((*Z*)-6-carbamoyl-2-((4-ethyl-2-methyloxazole-5-carbonyl)imino)thiazolo[4,5-*b*]pyridin-3(2*H*)-yl)but-2-en-1-yl)carbamate (390 mg, 0.86 mmol) and HCl (4 M in dioxane, 6 mL, 6 mmol) was stirred at room temperature for 6 h. The mixture was concentrated in vacuo to afford (*E*)-4-((*Z*)-6-carbamoyl-2-((4-ethyl-2-methyloxazole-5-carbonyl)imino)thiazolo-[4,5-*b*]pyridin-3(2*H*)-yl)but-2-en-1-aminium chloride (390 mg, 100% yield) as a brown solid. ^{1}H NMR (400 MHz, DMSO-d_6): δ 9.00 (d, J = 2.1 Hz, 1H), 8.82 (d, J = 1.9 Hz, 1H), 8.29 (s, 1H), 8.04 (s, 2H), 7.66 (s, 1H), 6.12−6.06 (m, 1H), 5.74−5.69 (m, 1H), 5.11 (d, J = 5.6 Hz, 2H), 3.41 (dd, J = 10.5, 4.9 Hz, 2H), 3.02 (t, J = 7.5 Hz, 2H), 1.24 (t, J = 7.5 Hz, 3H). ESI-MS: $C_{18}H_{21}N_6O_3S$ (M + H), calcd 401.13; found, 401.20.

N-((Z)-3-((E)-4-((2-(3-((tert-Butyldimethylsilyl)oxy)propoxy)-4-carbamoyl-6-nitrophenyl)amino)but-2-en-1-yl)-6-carbamoylthiazolo[4,5-b]pyridin-2(3H)-ylidene)-4-ethyl-2-methyloxazole-5-carboxamide. To a stirred solution of (*E*)-4-((*Z*)-6-carbamoyl-2-((4-ethyl-2-methyloxazole-5-carbonyl)imino)thiazolo-[4,5-*b*]pyridin-3(2*H*)-yl)but-2-en-1-aminium chloride (390 mg, 0.89 mmol) in DMF (10 mL) was added Et_3N (0.63 mL, 4.46 mmol), and the mixture was stirred for 5 min. 3-(3-((*tert*-butyldimethylsilyl)oxy)-propoxy)-4-chloro-5-nitrobenzamide (432 mg, 1.16 mmol) was added, and the mixture was stirred at room temperature for 16 h and then poured over water and stirred for 5 min. The resulting solid was filtered and purified over silica gel (DCM/MeOH 20:1 v/v) to afford *N*-((*Z*)-3-((*E*)-4-((2-(3-((*tert*-butyldimethylsilyl)oxy)-propoxy)-4-carbamoyl-6-nitrophenyl)amino)but-2-en-1-yl)-6-carbamoylthiazolo[4,5-*b*]pyridin-2(3*H*)-ylidene)-4-ethyl-2-methyloxazole-5-carboxamide (350 mg, 52% yield) as a yellow solid. ^{1}H NMR (400 MHz, DMSO-d_6): δ 8.89 (d, J = 2.0 Hz, 1H), 8.71 (d, J = 2.0 Hz, 1H), 8.14 (s, 1H), 8.01 (d, J = 1.9 Hz, 1H), 7.90 (s, 1H), 7.63 (dd, J = 12.3, 6.0 Hz, 2H), 7.39 (d, J = 2.0 Hz, 1H), 7.25 (s, 1H), 5.79−5.66 (m, 2H), 4.98 (d, J = 4.8 Hz, 2H), 4.07 (dt, J = 5.2, 2.3 Hz, 2H), 3.93 (t, J = 6.0 Hz, 2H), 3.58 (t, J = 6.1 Hz, 2H), 2.87 (q, J = 7.5 Hz, 2H), 2.43 (s, 3H), 1.76 (q, J = 6.1 Hz, 2H), 1.10 (t, J = 7.6 Hz, 3H), 0.75 (s, 9H), −0.09 (s, 6H). ESI-MS: $C_{34}H_{45}N_8O_8SSi$ (M + H), calcd 753.28; found, 753.20.

N-((Z)-3-((E)-4-((2-Amino-6-(3-((tert-butyldimethylsilyl)oxy)-propoxy)-4-carbamoylphenyl)amino)but-2-en-1-yl)-6-carbamoylthiazolo[4,5-b]pyridin-2(3H)-ylidene)-4-ethyl-2-methyloxazole-5-carboxamide. To a stirred solution of *N*-((*Z*)-3-((*E*)-4-((2-(3-((*tert*-butyldimethylsilyl)oxy)propoxy)-4-carbamoyl-6-nitrophenyl)amino)but-2-en-1-yl)-6-carbamoylthiazolo[4,5-*b*]pyridin-2(3*H*)-ylidene)-4-ethyl-2-methyloxazole-5-carboxamide (350 mg, 0.46 mmol) in MeOH (20 mL) at 0 °C was added $Na_2S_2O_4$ (960 mg, 4.65 mmol) in water (10 mL) followed by NH_4OH (25% aqueous solution, 1.64 mL, 11.62 mmol). The mixture was stirred at room temperature for 4 h and then diluted in water and extracted with EtOAc. The combined organic layers were dried over Na_2SO_4 and concentrated in vacuo to afford *N*-((*Z*)-3-((*E*)-4-((2-amino-6-(3-((*tert*-butyldimethylsilyl)oxy)propoxy)-4-carbamoylphenyl)amino)-but-2-en-1-yl)-6-carbamoylthiazolo[4,5-*b*]pyridin-2(3*H*)-ylidene)-4-ethyl-2-methyloxazole-5-carboxamide (220 mg, 65% yield) as a brown solid. ^{1}H NMR (400 MHz, DMSO-d_6): δ 8.94 (d, J = 2.0 Hz, 1H), 8.76 (d, J = 2.0 Hz, 1H), 8.18 (s, 1H), 7.60 (d, J = 29.8 Hz, 2H), 6.94 (s, 1H), 6.80 (d, J = 1.8 Hz, 1H), 6.70 (d, J = 1.9 Hz, 1H), 5.92−5.77 (m, 2H), 5.04 (d, J = 5.0 Hz, 2H), 4.62 (s, 2H), 3.89 (t, J = 6.0 Hz, 2H), 3.62 (t, J = 6.2 Hz, 2H), 2.99 (q, J = 7.6 Hz, 2H), 2.48 (s, 3H), 1.75 (q, J = 6.0, 4.2 Hz, 2H), 1.18 (d, J = 7.7 Hz, 3H), 0.78 (s, 9H), −0.07 (s, 6H). ESI-MS: $C_{34}H_{47}N_8O_6SSi$ (M + H), calcd 723.30; found, 723.20.

N-((Z)-3-((E)-4-(2-Amino-5-carbamoyl-7-(3-hydroxypropoxy)-1H-benzo[d]imidazole-1-yl)but-2-en-1-yl)-6-carbamoylthiazolo-[4,5-b]pyridin-2(3H)-ylidene)-4-ethyl-2-methyloxazole-5-carboxamide. To a stirred solution of *N*-((*Z*)-3-((*E*)-4-((2-amino-6-(3-((*tert*-butyldimethylsilyl)oxy)propoxy)-4-carbamoylphenyl)amino)but-2-en-1-yl)-6-carbamoylthiazolo[4,5-*b*]pyridin-2(3*H*)-ylidene)-4-ethyl-2-methyloxazole-5-carboxamide (220 mg, 0.30 mmol) in MeOH (8 mL) was added BrCN (55 mg, 0.52 mmol). The mixture was stirred at room temperature for 20 h and then concentrated in vacuo to afford *N*-((*Z*)-3-((*E*)-4-(2-amino-5-carbamoyl-7-(3-hydroxypropoxy)-1*H*-benzo[*d*]imidazole-1-yl)but-2-en-1-yl)-6-carbamoylthiazolo[4,5-*b*]pyridin-2(3*H*)-ylidene)-4-ethyl-2-methyloxazole-5-carboxamide (200 mg, 91% yield) as a white solid. ^{1}H NMR (400 MHz, DMSO-d_6): δ 8.94 (d, J = 2.0 Hz, 1H), 8.78 (d, J = 2.0 Hz, 1H), 8.58 (s, 2H), 8.19 (s, 1H), 8.04 (s, 1H), 7.66 (s, 1H), 7.49−7.33 (m, 3H), 5.85 (qt, J = 15.7, 5.1 Hz, 2H), 5.05 (d, J = 5.1 Hz, 2H), 4.83 (d, J = 5.1 Hz, 2H), 4.07 (t, J = 6.4 Hz, 2H), 3.39 (d, J = 6.0 Hz, 2H), 2.77 (q, J = 7.5 Hz, 2H), 2.45 (s, 3H), 1.67 (p, J = 6.5 Hz, 2H), 1.02 (t, J = 7.5 Hz, 3H). ESI-MS: $C_{29}H_{32}N_9O_6S$ (M + H), calcd 634.21; found, 634.15.

N-(5-Carbamoyl-1-((E)-4-((Z)-6-carbamoyl-2-((4-ethyl-2-methyloxazole-5-carbonyl)imino)thiazolo[4,5-b]pyridin-3(2H)-yl)but-2-en-1-yl)-7-(3-hydroxypropoxy)-1H-benzo[d]imidazole-2-yl)-4-ethyl-2-methyloxazole-5-carboxamide, Compound ***34****.* To a stirred solution of *N*-((*Z*)-3-((*E*)-4-(2-amino-5-carbamoyl-7-(3-hydroxypropoxy)-1*H*-benzo[*d*]imidazole-1-yl)but-2-en-1-yl)-6-carbamoylthiazolo[4,5-*b*]pyridin-2(3*H*)-ylidene)-4-ethyl-2-methyloxazole-5-carboxamide (200 mg, 0.28 mmol) and 4-ethyl-2-methyloxazole-5-carboxylic acid (65 mg, 0.42 mmol) in DMF were added Et_3N (0.2 mL, 1.04 mmol) and benzotriazole-1-yl-oxy-tris-pyrrolidino-phosphonium hexafluorophosphate (PyBOP) (220 mg, 0.42 mmol). The mixture was stirred at room temperature for 16 h and then poured over water and stirred for 5 min. The resulting solid was filtered and dried and then stirred in $MeNH_2$ (33% in EtOH, 1 mL) to hydrolyze the undesired ester. The mixture was concentrated in vacuo, and the residue was purified by HPLC (ACN/water) to afford *N*-(5-carbamoyl-1-((*E*)-4-((*Z*)-6-carbamoyl-2-((4-ethyl-2-methyloxazole-5-carbonyl)imino)thiazolo[4,5-*b*]pyridin-3(2*H*)-yl)but-2-en-1-yl)-7-(3-hydroxypropoxy)-1*H*-benzo[*d*]imidazole-2-yl)-4-ethyl-2-methyloxazole-5-carboxamide, compound **34** (45 mg, 18% yield), as a white solid. ^{1}H NMR (400 MHz, DMSO-d_6): δ 8.88 (d, J = 2.0 Hz, 1H), 8.71 (d, J = 2.0 Hz, 1H), 8.14 (s, 1H), 7.92 (s, 1H), 7.59 (d, J = 12.5 Hz, 2H), 7.27 (s, 2H), 6.49 (s, 1H), 5.82 (dd, J = 21.6, 16.6 Hz, 2H), 4.99 (s, 2H), 4.86 (s, 2H), 4.05 (d, J = 6.7 Hz, 1H), 2.81−2.71 (m, 6H), 1.74−1.64 (m, 2H), 0.94 (td, J = 7.6, 3.6 Hz, 6H). ESI-MS: $C_{36}H_{39}N_{10}O_8S$ (M + H), calcd 771.26; found, 771.29.

Synthesis and Characterization of Compound 35. *3-Methoxy-4-nitrobenzamide.* To a stirred solution of 3-methoxy-4-nitrobenzoic acid (30 g, 152.3 mmol) in DMF (300 mL) at 0 °C were added HATU (86.8 g, 228.4 mmol) and DIPEA (80 mL, 456.8 mmol), and the mixture was stirred for 10 min. Then, NH_4Cl (24.4 g, 456.8 mmol) was added, and the mixture was warmed to room temperature and stirred for 3 h. The mixture was poured over ice water, and the resulting precipitate was filtered and dried to afford 3-methoxy-4-nitrobenzamide (25.0 g, 83% yield) as a white solid. ^{1}H NMR (400 MHz, DMSO-d_6): δ 8.23 (s, 1H), 7.94 (d, J = 8.3 Hz, 1H), 7.75 (d, J = 1.7 Hz, 1H), 7.70 (s, 1H), 7.57 (dd, J = 8.4, 1.7 Hz, 1H), 3.98 (s, 3H). ESI-MS: $C_8H_9N_2O_4$ (M + H), calcd 197.05; found, 197.05. ESI-MS: $C_8H_9N_2O_4$ (M + H), calcd 197.05; found, 197.05.

3-Hydroxy-4-nitrobenzamide. To a stirred solution of 3-methoxy-4-nitrobenzamide (15 g, 75.6 mmol) in DCM (150 mL) under nitrogen at 0 °C was added BBr_3 (1 M in DCM, 383 mL, 382.6 mmol), and the mixture was allowed to warm to room temperature and stirred for 16 h. The mixture was then poured over ice water, and the resulting precipitate was filtered and dried to afford 3-hydroxy-4-nitrobenzamide (8 g, 56% yield) as a yellow solid. ^{1}H NMR (400 MHz, DMSO-d_6): δ 11.16 (s, 1H), 8.11 (s, 1H), 7.89 (d, J = 8.6 Hz, 1H), 7.59 (s, 1H), 7.52 (d, J = 1.7 Hz, 1H), 7.36 (dd, J = 8.5, 1.8 Hz, 1H). ESI-MS: $C_7H_7N_2O_4$ (M + H), calcd 183.03; found, 183.05.

3-(3-((tert-Butyldimethylsilyl)oxy)propoxy)-4-nitrobenzamide. To a stirred solution of 3-hydroxy-4-nitrobenzamide (8 g, 43.9 mmol) in DMF (120 mL) were added potassium carbonate (12.14 g, 87.9 mmol) and (3-bromopropoxy) (*tert*-butyl)dimethylsilane (14.45 g, 57.1 mmol), and the mixture was heated to 100 °C and stirred for 2 h. The mixture was cooled to room temperature and poured over ice water, and the resulting precipitate was filtered and dried to afford 3-

https://doi.org/10.1021/acs.jmedchem.3c00907
J. Med. Chem. 2023, 66, 10715−10733

(3-((*tert*-butyldimethylsilyl)oxy)propoxy)-4-nitrobenzamide (9 g, 57% yield) as a brown solid. ^{1}H NMR (400 MHz, DMSO-d_6): δ 8.83 (s, 1H), 8.52 (d, J = 8.4 Hz, 1H), 8.31 (d, J = 18.8 Hz, 2H), 8.15 (d, J = 8.4 Hz, 1H), 4.85 (t, J = 5.8 Hz, 2H), 4.33 (t, J = 6.1 Hz, 2H), 3.93 (s, 2H), 1.42 (s, 9H), 0.58 (s, 6H). ESI-MS: $C_{16}H_{27}N_2O_5Si$ (M + H), calcd 355.16.

4-Amino-3-(3-((tert-butyldimethylsilyl)oxy)propoxy)benzamide. To a stirred solution of 3-(3-((*tert*-butyldimethylsilyl)oxy)propoxy)-4-nitrobenzamide (9 g, 25.4 mmol) in MeOH (100 mL) was added Pd/C (1.8 g, 20% w/w), and the mixture was stirred for 16 h under a hydrogen atmosphere. The mixture was filtered over Celite and concentrated in vacuo to afford 4-amino-3-(3-((*tert*-butyldimethylsilyl)oxy)propoxy)benzamide (7.5 g, 91% yield) as a yellow solid. ^{1}H NMR (400 MHz, DMSO-d_6): δ 7.57 (s, 1H), 7.35−7.24 (m, 2H), 6.96−6.79 (m, 1H), 6.59 (d, J = 8.1 Hz, 1H), 5.20 (s, 2H), 4.03 (t, J = 6.1 Hz, 2H), 3.79 (t, J = 6.1 Hz, 2H), 1.92 (p, J = 6.2 Hz, 2H), 0.86 (s, 9H). ESI-MS: $C_{16}H_{29}N_2O_3Si$ (M + H), calcd 325.19; found, 325.20.

tert-Butyl (E)-(4-((2-(3-((tert-Butyldimethylsilyl)oxy)propoxy)-4-carbamoylphenyl)amino)but-2-en-1-yl)carbamate. To a stirred solution of 4-amino-3-(3-((*tert*-butyldimethylsilyl)oxy)propoxy)-benzamide (7.5 g, 23.1 mmol) in DMF (110 mL) were added potassium carbonate (7.79 g, 34.7 mmol) and *tert*-butyl (*E*)-(4-bromobut-2-en-1-yl)carbamate (6.36 g, 25.4 mmol), and the mixture was heated to 100 °C and stirred for 16 h. The mixture was cooled to room temperature and poured over ice water, and the resulting precipitate was filtered and dried. Purification over silica gel (DCM/MeOH 20:1 v/v) afforded *tert*-butyl (*E*)-(4-((2-(3-((*tert*-butyldimethylsilyl)oxy)propoxy)-4-carbamoylphenyl)amino)but-2-en-1-yl)carbamate (7 g, 61% yield) as a white solid. ^{1}H NMR (400 MHz, DMSO-d_6): δ 5.56−5.38 (m, 2H), 3.99 (dt, J = 9.5, 6.0 Hz, 2H), 3.76 (t, J = 6.0 Hz, 2H), 3.47 (d, J = 6.1 Hz, 1H), 1.89 (h, J = 6.2 Hz, 2H), 1.36−1.31 (m, 6H), 1.26−1.15 (m, 2H), 0.81 (d, J = 1.6 Hz, 9H). ESI-MS: $C_{25}H_{44}N_3O_5Si$ (M + H), calcd 494.30; found, 494.30.

tert-Butyl (E)-(4-(6-carbamoyl-4-(3-hydroxypropoxy)-2-iminobenzo[d]thiazol-3(2H)-yl)but-2-en-1-yl)carbamate. To a stirred solution of *tert*-butyl (*E*)-(4-((2-(3-((*tert*-butyldimethylsilyl)-oxy)propoxy)-4-carbamoylphenyl)amino)but-2-en-1-yl)carbamate (7 g, 14.2 mmol) in acetic acid (70 mL) at 0 °C was added potassium thiocyanate (5.51 g, 56.8 mmol), and the mixture was stirred for 20 min. Then, Br_2 (2.49 g, 15.6 mmol) dissolved in acetic acid (25 mL) was added dropwise, and the mixture was allowed to warm to room temperature and stirred for 16 h. The mixture was poured over ice water and solids removed by filtration. The filtrate was extracted with EtOAc and the organic layer discarded. The aqueous layer was basified with aqueous ammonia and extracted with EtOAc, and the combined organic layers were dried over Na_2SO_4 and concentrated in vacuo to afford *tert*-butyl (*E*)-(4-(6-carbamoyl-4-(3-hydroxypropoxy)-2-iminobenzo[*d*]thiazol-3(2*H*)-yl)but-2-en-1-yl)carbamate (3 g, 29% yield) as a white solid. ^{1}H NMR (400 MHz, DMSO-d_6): δ 7.83 (s, 1H), 7.49 (d, J = 1.5 Hz, 1H), 7.37 (d, J = 1.6 Hz, 1H), 7.23 (s, 1H), 6.89 (t, J = 6.0 Hz, 1H), 5.65−5.53 (m, 1H), 5.44 (ddt, J = 15.7, 10.7, 5.4 Hz, 1H), 4.76 (d, J = 5.4 Hz, 2H), 4.13−4.06 (m, 3H), 3.55 (dd, J = 6.5, 4.9 Hz, 2H), 3.44 (t, J = 5.4 Hz, 2H), 1.91−1.84 (m, 2H), 1.30 (s, 9H). ESI-MS: $C_{20}H_{29}N_4O_5S$ (M + H), calcd 437.18; found, 437.10.

tert-Butyl ((E)-4-((Z)-6-carbamoyl-2-((4-ethyl-2-methyloxazole-5-carbonyl)imino)-4-(3-hydroxypropoxy)benzo[d]thiazol-3(2H)-yl)-but-2-en-1-yl)carbamate. To a stirred solution of *tert*-butyl (*E*)-(4-(6-carbamoyl-4-(3-hydroxypropoxy)-2-iminobenzo[*d*]thiazol-3(2*H*)-yl)but-2-en-1-yl)carbamate (6 g, 13.8 mmol) and 4-ethyl-2-methyl-oxazole-5-carboxylic acid (2.56 g, 16.5 mmol) in DMF (60 mL) were added DIPEA (12 mL, 68.8 mmol) and HATU (7.84 g, 20.6 mmol), and the mixture was stirred at room temperature for 3 h. The mixture was poured over ice water, and the resulting solid was filtered and dried. Purification over silica gel (DCM/MeOH 20:1 v/v) afforded *tert*-butyl ((*E*)-4-((*Z*)-6-carbamoyl-2-((4-ethyl-2-methyloxazole-5-carbonyl)imino)-4-(3-hydroxypropoxy)benzo[*d*]thiazol-3(2*H*)-yl)-but-2-en-1-yl)carbamate (4 g, 50% yield) as a white solid. ^{1}H NMR (400 MHz, DMSO-d_6): δ 8.10 (s, 1H), 7.99 (s, 1H), 7.61 (s, 1H), 7.49 (s, 1H), 6.92 (t, J = 5.9 Hz, 1H), 5.78 (dt, J = 15.7, 5.8 Hz, 1H), 5.57 (dt, J = 15.7, 5.4 Hz, 1H), 5.34 (d, J = 5.6 Hz, 2H), 4.27 (t, J = 6.3 Hz, 2H), 3.63 (q, J = 5.8 Hz, 2H), 3.50 (d, J = 11.4 Hz, 2H), 3.00 (q, J = 7.5 Hz, 2H), 2.47 (s, 4H), 2.00 (p, J = 6.2 Hz, 2H), 1.31 (s, 9H), 1.21 (t, J = 7.5 Hz, 4H). ESI-MS: $C_{27}H_{36}N_5O_7S$ (M + H), calcd 574.23; found, 574.25.

N-((Z)-3-((E)-4-Aminobut-2-en-1-yl)-6-carbamoyl-4-(3-hydroxypropoxy)benzo[d]thiazol-2(3H)-ylidene)-4-ethyl-2-methyl-oxazole-5-carboxamide. *tert*-Butyl ((*E*)-4-((*Z*)-6-carbamoyl-2-((4-ethyl-2-methyloxazole-5-carbonyl)imino)-4-(3-hydroxypropoxy)-benzo[*d*]thiazol-3(2*H*)-yl)but-2-en-1-yl)carbamate (350 mg, 0.610 mmol) was stirred in HCl (4 M in dioxane, 10 mL) at 30 °C for 1 h. The mixture was concentrated in vacuo to afford *N*-((Z)-3-((*E*)-4-aminobut-2-en-1-yl)-6-carbamoyl-4-(3-hydroxypropoxy)benzo[*d*]-thiazol-2(3*H*)-ylidene)-4-ethyl-2-methyloxazole-5-carboxamide (311 mg, 100% yield) as a white solid. ^{1}H NMR (400 MHz, DMSO-d_6): δ 8.12 (s, 1H), 8.06−7.91 (m, 3H), 7.67−7.59 (m, 1H), 7.46 (s, 1H), 6.06 (dt, J = 15.9, 5.3 Hz, 1H), 5.56 (dd, J = 14.5, 7.3 Hz, 1H), 5.36 (d, J = 5.3 Hz, 2H), 4.25 (t, J = 6.4 Hz, 2H), 3.59 (t, J = 6.1 Hz, 2H), 3.43−3.31 (m, 2H), 2.96 (q, J = 7.6 Hz, 2H), 2.44 (s, 3H), 1.98 (p, J = 6.4 Hz, 2H), 1.18 (t, J = 7.4 Hz, 3H). ESI-MS: $C_{22}H_{28}N_5O_5S$ (M + H), calcd 474.17; found, 474.20.

6-(((E)-4-((Z)-6-Carbamoyl-2-((4-ethyl-2-methyloxazole-5-carbonyl)imino)-4-(3-hydroxypropoxy)benzo[d]thiazol-3(2H)-yl)-but-2-en-1-yl)amino)-5-nitronicotinic Acid. To a stirred solution of 6-chloro-5-nitronicotinic acid (115 mg, 0.569 mmol) in ACN (10 mL) were added *N*-((*Z*)-3-((*E*)-4-aminobut-2-en-1-yl)-6-carbamoyl-4-(3-hydroxypropoxy)benzo[*d*]thiazol-2(3*H*)-ylidene)-4-ethyl-2-methyloxazole-5-carboxamide (347 mg, 0.682 mmol) and Et_3N (0.40 mL, 2.85 mmol), and the mixture was heated to 100 °C and stirred for 16 h. The mixture was cooled to room temperature, and the resulting solid was filtered and washed with CH_3CN to afford 6-(((*E*)-4-((*Z*)-6-carbamoyl-2-((4-ethyl-2-methyloxazole-5-carbonyl)-imino)-4-(3-hydroxypropoxy)benzo[*d*]thiazol-3(2*H*)-yl)but-2-en-1-yl)amino)-5-nitronicotinic acid (200 mg, 54% yield) as a yellow solid. ^{1}H NMR (400 MHz, DMSO-d_6): δ 8.89−8.75 (m, 2H), 8.68 (s, 1H), 8.09 (s, 1H), 7.97 (s, 1H), 7.59 (s, 1H), 7.45 (s, 1H), 5.89 (dt, J = 15.8, 5.4 Hz, 1H), 5.73 (dt, J = 15.7, 5.3 Hz, 1H), 5.34 (d, J = 5.3 Hz, 2H), 4.21 (d, J = 6.6 Hz, 2H), 3.53 (t, J = 6.1 Hz, 2H), 2.92 (q, J = 7.5 Hz, 2H), 2.84−2.77 (m, 2H), 1.87 (p, J = 6.4 Hz, 2H), 1.09 (q, J = 7.4 Hz, 6H). ESI-MS: $C_{28}H_{30}N_7O_9S$ (M + H), calcd 640.17; found, 640.20.

N-((Z)-6-Carbamoyl-3-((E)-4-((5-carbamoyl-3-nitropyridin-2-yl)-amino)but-2-en-1-yl)-4-(3-hydroxypropoxy)benzo[d]thiazol-2(3H)-ylidene)-4-ethyl-2-methyloxazole-5-carboxamide. To a stirred solution of 6-(((*E*)-4-((*Z*)-6-carbamoyl-2-((4-ethyl-2-methyloxazole-5-carbonyl)imino)-4-(3-hydroxypropoxy)benzo[*d*]thiazol-3(2*H*)-yl)-but-2-en-1-yl)amino)-5-nitronicotinic acid (200 mg, 0.312 mmol) in DMF (10 mL) were added NH_4Cl (33 mg, 0.624 mmol), HATU (177 mg, 0.468 mmol), and DIPEA (0.27 mL, 1.56 mmol), and the mixture was heated to 30 °C and stirred for 16 h. The mixture was cooled to room temperature and poured over ice water, and the resulting precipitate was filtered and dried to afford *N*-((*Z*)-6-carbamoyl-3-((*E*)-4-((5-carbamoyl-3-nitropyridin-2-yl)amino)but-2-en-1-yl)-4-(3-hydroxypropoxy)benzo[*d*]thiazol-2(3*H*)-ylidene)-4-ethyl-2-methyloxazole-5-carboxamide (200 mg, 99% yield) as a yellow solid. ^{1}H NMR (400 MHz, DMSO-d_6): δ 8.85 (d, J = 8.1 Hz, 3H), 8.07 (s, 2H), 7.97 (d, J = 10.9 Hz, 1H), 7.60 (s, 1H), 7.46 (s, 2H), 5.90 (dt, J = 15.9, 5.3 Hz, 1H), 5.75 (dd, J = 13.0, 7.7 Hz, 1H), 5.34 (d, J = 5.3 Hz, 2H), 4.21 (q, J = 6.2 Hz, 4H), 3.54 (q, J = 5.7 Hz, 2H), 2.90 (d, J = 3.8 Hz, 2H), 2.45 (s, 3H), 1.87 (p, J = 6.3 Hz, 2H), 1.10 (t, J = 7.5 Hz, 3H). ESI-MS: $C_{28}H_{31}N_8O_8S$ (M + H), calcd 639.19; found, 639.20.

N-((Z)-3-((E)-4-((3-Amino-5-carbamoylpyridin-2-yl)amino)but-2-en-1-yl)-6-carbamoyl-4-(3-hydroxypropoxy)benzo[d]thiazol-2(3H)-ylidene)-4-ethyl-2-methyloxazole-5-carboxamide. To a stirred solution of *N*-((*Z*)-6-carbamoyl-3-((*E*)-4-((5-carbamoyl-3-nitropyridin-2-yl)amino)but-2-en-1-yl)-4-(3-hydroxypropoxy)benzo[*d*]thiazol-2(3*H*)-ylidene)-4-ethyl-2-methyloxazole-5-carboxamide (200 mg, 0.313 mmol) in concentrated HCl (10 mL) at 0 °C was added $SnCl_2$ (272 mg, 1.57 mmol), and the mixture was stirred for 1 h. The

https://doi.org/10.1021/acs.jmedchem.3c00907
J. Med. Chem. 2023, 66, 10715−10733

mixture was quenched with 6 N NaOH, and the resulting precipitate was filtered to afford *N*-((*Z*)-3-((*E*)-4-((3-amino-5-carbamoylpyridin-2-yl)amino)but-2-en-1-yl)-6-carbamoyl-4-(3-hydroxypropoxy)benzo[*d*]thiazol-2(3*H*)-ylidene)-4-ethyl-2-methyloxazole-5-carboxamide (120 mg, 63% yield) as a white solid. ^{1}H NMR (400 MHz, DMSO-d_6): δ 8.07 (s, 1H), 7.92 (d, J = 26.0 Hz, 2H), 7.51 (d, J = 47.5 Hz, 3H), 7.06 (s, 1H), 6.86 (s, 1H), 6.15 (s, 1H), 5.89−5.71 (m, 2H), 5.31 (s, 2H), 4.72 (s, 2H), 4.20 (t, J = 6.4 Hz, 2H), 3.97 (s, 2H), 3.53 (s, 2H), 2.90 (q, J = 7.6 Hz, 3H), 1.91−1.78 (m, 2H), 1.09 (t, J = 7.7 Hz, 3H). ESI-MS: $C_{28}H_{33}N_8O_6S$ (M + H), calcd 609.22; found, 609.20.

N-(6-Carbamoyl-3-((E)-4-((Z)-6-carbamoyl-2-((4-ethyl-2-methyloxazole-5-carbonyl)imino)-4-(3-hydroxypropoxy)benzo[d]thiazol-3(2H)-yl)but-2-en-1-yl)-3H-imidazo[4,5-b]pyridin-2-yl)-4-ethyl-2-methyloxazole-5-carboxamide, Compound ***35***. To a stirred solution of *N*-((*Z*)-3-((*E*)-4-((3-amino-5-carbamoylpyridin-2-yl)amino)but-2-en-1-yl)-6-carbamoyl-4-(3-hydroxypropoxy)benzo[*d*]thiazol-2(3*H*)-ylidene)-4-ethyl-2-methyloxazole-5-carboxamide (120 mg, 0.197 mmol) in DMF (5 mL) at 0 °C was added 4-ethyl-2-methyloxazole-5-carbonyl isothiocyanate (1.48 mL, 0.591 mmol), and the mixture was stirred for 10 min. Then, EDC·HCl (94 mg, 0.492 mmol) and Et_3N (0.14 mL, 0.985 mmol) were added, and the mixture was allowed to warm to room temperature and was stirred for 16 h. The mixture was concentrated in vacuo and the residue was diluted in EtOAc and washed with water. The organic layer was dried over Na_2SO_4 and concentrated in vacuo. Purification by reverse-phase HPLC (ACN/water) afforded *N*-(6-carbamoyl-3-((*E*)-4-((*Z*)-6-carbamoyl-2-((4-ethyl-2-methyloxazole-5-carbonyl)imino)-4-(3-hydroxypropoxy)benzo[*d*]thiazol-3(2*H*)-yl)but-2-en-1-yl)-3*H*-imidazo[4,5-*b*]pyridin-2-yl)-4-ethyl-2-methyloxazole-5-carboxamide, compound **35** (80 mg, 53% yield), as a white solid. ^{1}H NMR (400 MHz, DMSO-d_6): δ 12.71 (s, 1H), 8.65 (d, J = 1.9 Hz, 1H), 8.14−8.05 (m, 2H), 8.02 (s, 1H), 7.92 (d, J = 1.4 Hz, 1H), 7.53−7.45 (m, 2H), 7.43 (s, 1H), 5.84 (dt, J = 15.7, 5.1 Hz, 1H), 5.72 (dt, J = 15.6, 5.4 Hz, 1H), 5.26 (d, J = 5.0 Hz, 2H), 4.70 (d, J = 5.3 Hz, 2H), 4.09 (t, J = 6.4 Hz, 2H), 3.42 (s, 2H), 2.82−2.70 (m, 4H), 2.37 (d, J = 9.8 Hz, 6H), 1.72 (p, J = 6.2 Hz, 2H), 0.94 (dt, J = 17.7, 7.5 Hz, 6H). ESI-MS: $C_{36}H_{39}N_{10}O_8S$ (M + H), calcd 771.26; found, 771.30.

Synthesis of PEG8-Bisglucamine-Based Scaffolds (Precursors to ADCs 36−39, 42, and 47). *(E)-3-((5-Carbamoyl-1-(4-(5-carbamoyl-2-(1-ethyl-3-methyl-1H-pyrazole-5-carboxamido)-7-methoxy-1H-benzo[d]imidazole-1-yl)but-2-en-1-yl)-2-(1-ethyl-3-methyl-1H-pyrazole-5-carboxamido)-1H-benzo[d]imidazole-7-yl)oxy)propyl (tert-Butoxycarbonyl)-L-alaninate.* To a mixture of compound **6** (0.5 g, 0.64 mmol), Boc-L-alanine (0.242 g, 1.28 mmol), DMAP (7.8 mg, 0.064 mmol), and DCC (0.264 g, 1.28 mmol) was added DMF (2 mL). The suspension was stirred overnight at room temperature and then, the solution was concentrated, and the residue was purified on silica gel (0−40% MeOH in DCM) to give the title compound as a light-yellow solid (0.52 g, 85% yield). ESI-MS *m/z*: calcd for $C_{46}H_{58}N_{13}O_{10}$ $[M + H]^+$: 952.4; found, 952.4.

(E)-3-((5-Carbamoyl-1-(4-(5-carbamoyl-2-(1-ethyl-3-methyl-1H-pyrazole-5-carboxamido)-7-methoxy-1H-benzo[d]imidazole-1-yl)but-2-en-1-yl)-2-(1-ethyl-3-methyl-1H-pyrazole-5-carboxamido)-1H-benzo[d]imidazole-7-yl)oxy)propyl L-Alaninate. To a suspension of (*E*)-3-((5-carbamoyl-1-(4-(5-carbamoyl-2-(1-ethyl-3-methyl-1*H*-pyrazole-5-carboxamido)-7-methoxy-1*H*-benzo[*d*]imidazole-1-yl)but-2-en-1-yl)-2-(1-ethyl-3-methyl-1*H*-pyrazole-5-carboxamido)-1*H*-benzo[*d*]imidazole-7-yl)oxy)propyl (*tert*-butoxycarbonyl)-L-alaninate (0.52 g, 0.55 mmol) in dioxane (10 mL) was added 4 N HCl (2 mL, 8.19 mmol). The reaction mixture was stirred at room temperature for 2 h and then, the suspension was concentrated and used without further purification in the next step. The title compound was obtained as a white solid. ESI-MS *m/z*: calcd for $C_{41}H_{50}N_{13}O_8$ [M + H]: 852.4; found, 852.3.

(E)-3-((5-Carbamoyl-1-(4-(5-carbamoyl-2-(1-ethyl-3-methyl-1H-pyrazole-5-carboxamido)-7-methoxy-1H-benzo[d]imidazole-1-yl)but-2-en-1-yl)-2-(1-ethyl-3-methyl-1H-pyrazole-5-carboxamido)-1H-benzo[d]imidazole-7-yl)oxy)propyl (2,2-Dimethyl-4-oxo-3,8,11-trioxa-5-azatetradecan-14-oyl)-L-alaninate. To a solution of (*E*)-3-((5-carbamoyl-1-(4-(5-carbamoyl-2-(1-ethyl-3-methyl-1*H*-pyrazole-5-carboxamido)-7-methoxy-1*H*-benzo[*d*]imidazole-1-yl)but-2-en-1-yl)-2-(1-ethyl-3-methyl-1*H*-pyrazole-5-carboxamido)-1*H*-benzo[*d*]imidazole-7-yl)oxy)propyl L-alaninate (0.586 g, 0.661 mmol) in DMF (5 mL) was added 2,2-dimethyl-4-oxo-3,8,11-trioxa-5-azatetradecan-14-oic acid (0.202 g, 0.727 mmol), followed by DIPEA (0.230 mL, 1.322 mmol). The reaction mixture was stirred at room temperature for 5 min, and then HATU (0.376 g, 0.992 mmol) and HOBt (0.153 g, 0.992 mmol) were added. The reaction mixture was stirred at room temperature for 2 h. An additional aliquot of DIPEA (0.460 mL, 2.6 mmol) was added. After another 1 h, the reaction mixture was concentrated to an oil. The residue was purified over silica gel (0−40% MeOH in DCM) to afford the title compound (0.9 g, >95% yield) as a white solid. ESI-MS *m/z*: calcd for $C_{53}H_{71}N_{14}O_{13}$ $[M + H]^+$: 1111.5; found, 1111.5.

(E)-3-((5-Carbamoyl-1-(4-(5-carbamoyl-2-(1-ethyl-3-methyl-1H-pyrazole-5-carboxamido)-7-methoxy-1H-benzo[d]imidazole-1-yl)but-2-en-1-yl)-2-(1-ethyl-3-methyl-1H-pyrazole-5-carboxamido)-1H-benzo[d]imidazole-7-yl)oxy)propyl (3-(2-(2-Aminoethoxy)ethoxy)propanoyl)-L-alaninate. To a suspension of (*E*)-3-((5-carbamoyl-1-(4-(5-carbamoyl-2-(1-ethyl-3-methyl-1*H*-pyrazole-5-carboxamido)-7-methoxy-1*H*-benzo[*d*]imidazole-1-yl)but-2-en-1-yl)-2-(1-ethyl-3-methyl-1*H*-pyrazole-5-carboxamido)-1*H*-benzo[*d*]imidazole-7-yl)oxy)propyl (2,2-dimethyl-4-oxo-3,8,11-trioxa-5-azatetradecan-14-oyl)-L-alaninate (0.9 g, 0.810 mmol) in dioxane (10 mL) was added 4 N HCl (3.04 mL, 12.15 mmol). The reaction mixture was stirred at room temperature for 1.5 h. The suspension was concentrated to afford the title compound as a colorless solid (0.56 g, 66.0% yield). ESI-MS calcd for $C_{48}H_{63}N_{14}O_{11}$ $[M + H]^+$: 1011.5; found, 1011.4.

3-((5-Carbamoyl-1-((E)-4-(5-carbamoyl-2-(1-ethyl-3-methyl-1H-pyrazole-5-carboxamido)-7-methoxy-1H-benzo[d]imidazole-1-yl)but-2-en-1-yl)-2-(1-ethyl-3-methyl-1H-pyrazole-5-carboxamido)-1H-benzo[d]imidazole-7-yl)oxy)propyl ((S)-1-(2,5-Dioxo-2,5-dihydro-1H-pyrrol-1-yl)-2,7-dioxo-4-((2-oxo-2-((2-oxo-2-((2-oxo-2-(((3S,3S,3R,4R,4R)-3S,3R,4R,5R)-2,3,4,5,6-pentahydroxyhexyl)carbamoyl)-6,9,12,15,18,21,24,27-octaoxa-3,31,36-triazadotetracontyl)amino)ethyl)amino)ethyl)amino)ethyl)carbamoyl)-11,14-dioxa-3,8-diazaheptadecan-17-oyl)-L-alaninate, Precursor to ADC ***37***. To a solution of (4*S*,47*S*,53*S*,54*R*,55*R*,56*R*)-4-(2-(2,5-dioxo-2,5-dihydro-1*H*-pyrrol-1-yl)acetamido)-53,54,55,56,57-pentahydroxy-5,8,11,14,17,45,50-heptaoxo-47-(((2*S*,3*R*,4*R*,5*R*)-2,3,4,5,6-pentahydroxyhexyl)carbamoyl)-21,24,27,30,33,36,39,42-octaoxa-6,9,12,15,18,46,51-heptaazaheptapentacontanoic acid (100 mg, 0.072 mmol, prepared as described in PCT/US2018/06719) and (*E*)-3-((5-carbamoyl-1-(4-(5-carbamoyl-2-(1-ethyl-3-methyl-1*H*-pyrazole-5-carboxamido)-7-methoxy-1*H*-benzo[*d*]imidazole-1-yl)but-2-en-1-yl)-2-(1-ethyl-3-methyl-1*H*-pyrazole-5-carboxamido)-1*H*-benzo[*d*]imidazole-7-yl)oxy)propyl (3-(2-(2-aminoethoxy)ethoxy)propanoyl)-L-alaninate (72.7 mg, 0.072 mmol) in DMF (2 mL) were added PyBOP (37.5 mg, 0.072 mmol) and DIPEA (0.075 mL, 0.431 mmol). The reaction mixture was stirred at room temperature for 2 h, and then, the solution was concentrated, and the residue was purified by preparative HPLC (0−80% ACN in water) to afford the title compound (109 mg, 64% yield). ESI-MS *m/z*: calcd for $C_{103}H_{156}N_{24}O_{41}$ $[M + 2H]^{2+}$: 1192.5; found, 1192.5.

Precursors to ADC **36** and **38** were prepared in a similar fashion as described above, except for substituting the alanine unit. The precursor to ADC **39** was prepared in a similar fashion as described above, except for starting with payload **4** and substituting the PEG2 unit for an alanine unit. The precursors to ADC **42** and **47** were prepared similar to above, except for starting with payloads **15** and **19b**, respectively.

3-((5-Carbamoyl-1-((E)-4-(5-carbamoyl-2-(1-ethyl-3-methyl-1H-pyrazole-5-carboxamido)-7-methoxy-1H-benzo[d]imidazole-1-yl)but-2-en-1-yl)-2-(1-ethyl-3-methyl-1H-pyrazole-5-carboxamido)-1H-benzo[d]imidazole-7-yl)oxy)propyl (16S,59S,65S,66R,67R,68R)-16-(2-(2,5-Dioxo-2,5-dihydro-1H-pyrrol-1-yl)acetamido)-65,66,67,68,69-pentahydroxy-13,17,20,23,26,29,57,62-octaoxo-59-(((2S,3R,4R,5R)-2,3,4,5,6-Pentahydroxyhexyl)carbamoyl)-3,6,9,33,36,39,42,45,48,51,54-undecaoxa-12,18,21,24,27,30,58,63-

https://doi.org/10.1021/acs.jmedchem.3c00907
J. Med. Chem. 2023, 66, 10715−10733

octaazanonahexacontanoate, Precursor to ADC ***36***. $C_{101}H_{153}N_{23}O_{41}$ $[M + 2H]^{2+}$: 1172.53; found, 1172.55.

3-((5-Carbamoyl-1-((E)-4-(5-carbamoyl-2-(1-ethyl-3-methyl-1H-pyrazole-5-carboxamido)-7-methoxy-1H-benzo[d]imidazole-1-yl)-but-2-en-1-yl)-2-(1-ethyl-3-methyl-1H-pyrazole-5-carboxamido)-1H-benzo[d]imidazole-7-yl)oxy)propyl ((S)-1-(2,5-Dioxo-2,5-dihydro-1H-pyrrol-1-yl)-2,7-dioxo-4-((2-oxo-2-((2-oxo-2-((2-oxo-2-(((32S,38S,39R,40R,41R)-38,39,40,41,42-pentahydroxy-2,30,35-trioxo-32-(((2S,3R,4R,5R)-2,3,4,5,6-pentahydroxyhexyl)carbamoyl)-6,9,12,15,18,21,24,27-octaoxa-3,31,36-triazadotetracontyl)amino)-ethyl)amino)ethyl)amino)ethyl)carbamoyl)-11,14-dioxa-3,8-diazaheptadecan-17-oyl)-L-valinate, Precursor to ADC ***38***. $C_{105}H_{160}N_{24}O_{41}$ $[M + 2H]^{2+}$: 1207.06; found, 1207.08.

(S)-2-((42S,47S,50S)-55-((5-Carbamoyl-1-((E)-4-(5-carbamoyl-2-(1-ethyl-3-methyl-1H-pyrazole-5-carboxamido)-7-methoxy-1H-benzo[d]imidazole-1-yl)but-2-en-1-yl)-2-(1-ethyl-3-methyl-1H-pyrazole-5-carboxamido)-1H-benzo[d]imidazole-7-yl)oxy)-42-(2-(2,5-dioxo-2,5-dihydro-1H-pyrrol-1-yl)acetamido)-47,50-dimethyl-29,32,35,38,41,45,48,51-octaoxo-4,7,10,13,16,19,22,25-octaoxa-28,31,34,37,40,46,49,52-octaazapentapentacontanamido)-N1,N5-bis((2S,3R,4R,5R)-2,3,4,5,6-pentahydroxyhexyl)pentanediamide, Precursor to ADC ***39***. ESI-MS *m/z*: calcd for $C_{99}H_{149}N_{25}O_{38}$ $[M + 2H]^{2+}$: calcd 1148.0; found, 1148.4.

3-((5-Carbamoyl-1-((E)-4-(5-carbamoyl-2-(4-ethyl-2-methyloxazole-5-carboxamido)-7-methoxy-1H-benzo[d]imidazole-1-yl)but-2-en-1-yl)-2-(4-ethyl-2-methyloxazole-5-carboxamido)-1H-benzo[d]imidazole-7-yl)oxy)propyl ((S)-1-(2,5-Dioxo-2,5-dihydro-1H-pyrrol-1-yl)-2,7-dioxo-4-((2-oxo-2-((2-oxo-2-((2-oxo-2-(((32S,38S,39R,40R,41R)-38,39,40,41,42-pentahydroxy-2,30,35-trioxo-32-(((2S,3R,4R,5R)-2,3,4,5,6-pentahydroxyhexyl)carbamoyl)-6,9,12,15,18,21,24,27-octaoxa-3,31,36-triazadotetracontyl)amino)-ethyl)amino)ethyl)amino)ethyl)carbamoyl)-11,14-dioxa-3,8-diazaheptadecan-17-oyl)-L-alaninate, Precursor to ADC ***42***. ESI-MS *m/z*: calcd for $C_{103}H_{154}N_{22}O_{43}$ $[M + 2H]^{2+}$: 1193.52; found, 1193.48.

3-((5-Carbamoyl-1-((E)-4-(6-carbamoyl-2-(4-ethyl-2-methyloxazole-5-carboxamido)-3H-imidazo[4,5-b]pyridin-3-yl)but-2-en-1-yl)-2-(4-ethyl-2-methyloxazole-5-carboxamido)-1H-benzo[d]imidazole-7-yl)oxy)propyl ((S)-1-(2,5-Dioxo-2,5-dihydro-1H-pyrrol-1-yl)-2,7-dioxo-4-((2-oxo-2-((2-oxo-2-((2-oxo-2-(((32S,38S,39R,40R,41R)-38,39,40,41,42-pentahydroxy-2,30,35-trioxo-32-(((2S,3R,4R,5R)-2,3,4,5,6-pentahydroxyhexyl)carbamoyl)-6,9,12,15,18,21,24,27-octaoxa-3,31,36-triazadotetracontyl)amino)-ethyl)amino)ethyl)amino)ethyl)carbamoyl)-11,14-dioxa-3,8-diazaheptadecan-17-oyl)-L-alaninate, Precursor to ADC ***47***. ESI-MS *m/z*: calcd for $C_{101}H_{151}N_{23}O_{42}$ $[M + 2H]^{2+}$: 1179.02; found, 1179.21.

Synthesis of Non-Cleavable Scaffold and Corresponding Payload. *(E)-1-(4-(5-Carbamoyl-2-(1-ethyl-3-methyl-1H-pyrazole-5-carboxamido)-7-methoxy-1H-benzo[d]imidazole-1-yl)but-2-en-1-yl)-7-((1-(2,5-dioxo-2,5-dihydro-1H-pyrrol-1-yl)-21-oxo-3,6,9,12,15,18-hexaoxa-22-azapentacosan-25-yl)oxy)-2-(1-ethyl-3-methyl-1H-pyrazole-5-carboxamido)-1H-benzo[d]imidazole-5-carboxamide, Precursor to ADC 40.* To a solution of compound **4** (0.030 g, 0.038 mmol) in DMF (1.5 mL) was added *N*-ethyl-*N*-isopropylpropan-2-amine (0.067 mL, 0.385 mmol). The solution was stirred for 5 min at room temperature prior to the addition of 2,5-dioxopyrrolidin-1-yl 1-(2,5-dioxo-2,5-dihydro-1*H*-pyrrol-1-yl)-3,6,9,12,15,18-hexaoxahenicosan-21-oate (0.027 g, 0.050 mmol) in DMF (0.5 mL), and the reaction mixture was stirred at room temperature for 15 min. Then, acetic acid (0.1 mL) was added followed by purification on a preparative HPLC column (C18, 21.2 mm × 100 mm), 10−100% MeCN (0.1% HOAc) in H_2O (0.1% HOAc, 20 min gradient) to give the title compound (0.006 g, 13% yield). ESI-MS *m/z*: calcd for $C_{57}H_{75}N_{14}O_{15}$ $[M + H]^{+}$: calcd 1195.55; found, 1195.47.

S-(1-(25-((5-Carbamoyl-1-((E)-4-(5-carbamoyl-2-(1-ethyl-3-methyl-1H-pyrazole-5-carboxamido)-7-methoxy-1H-benzo[d]-imidazole-1-yl)but-2-en-1-yl)-2-(1-ethyl-3-methyl-1H-pyrazole-5-carboxamido)-1H-benzo[d]imidazole-7-yl)oxy)-21-oxo-3,6,9,12,15,18-hexaoxa-22-azapentacosyl)-2,5-dioxopyrrolidin-3-yl)-D-cysteine, Compound ***41***. To a suspension of the non-cleavable scaffold (0.019 g, 0.016 mmol) in DMSO (1 mL) was added a concentrated solution of L-cysteine (0.019 g, 0.159 mmol), and the mixture was stirred for 5 min. The mixture was directly loaded onto an RP column for purification to afford **41** as a white solid (0.010 g, 7.60 μmol, 47.8% yield). ESI-MS *m/z*: calcd for $C_{60}H_{82}N_{15}O_{17}S$ $[M + H]^{+}$, calcd 1316.57; found, 1316.63.

Synthesis of Low-MW Scaffolds (Precursors to ADCs 43−46 and 48). *(E)-3-((5-Carbamoyl-1-(4-(5-carbamoyl-2-(4-ethyl-2-methyloxazole-5-carboxamido)-7-methoxy-1H-benzo[d]-imidazole-1-yl)but-2-en-1-yl)-2-(4-ethyl-2-methyloxazole-5-carboxamido)-1H-benzo[d]imidazole-7-yl)oxy)propyl (tert-Butoxycarbonyl)-L-alaninate.* A mixture of **15** (85 mg, 0.109 mmol), (*tert*-butoxycarbonyl)-L-alanine (21 mg, 0.109 mmol), DCC (45 mg, 0.217 mmol), DMAP (13 mg, 0.109 mmol), and DMF (2.2 mL) was stirred at room temperature for 16 h. The reaction mixture was then diluted with DCM and absorbed onto silica gel. Purification over silica gel afforded the title compound (42.3 mg, 0.045 mmol, 41% yield). ESI-MS: $C_{46}H_{55}N_{11}O_{12}$ (M + H), calcd 954.40; found, 954.20.

(E)-3-((5-Carbamoyl-1-(4-(5-carbamoyl-2-(4-ethyl-2-methyloxazole-5-carboxamido)-7-methoxy-1H-benzo[d]imidazole-1-yl)but-2-en-1-yl)-2-(4-ethyl-2-methyloxazole-5-carboxamido)-1H-benzo-[d]imidazole-7-yl)oxy)propyl L-Alaninate. A solution of (*E*)-3-((5-carbamoyl-1-(4-(5-carbamoyl-2-(4-ethyl-2-methyloxazole-5-carboxamido)-7-methoxy-1*H*-benzo[*d*]imidazole-1-yl)but-2-en-1-yl)-2-(4-ethyl-2-methyloxazole-5-carboxamido)-1*H*-benzo[*d*]imidazole-7-yl)-oxy)propyl (*tert*-butoxycarbonyl)-L-alaninate (43 mg, 0.045 mmol), DCM (2.2 mL), and TFA (0.242 mL, 3.12 mmol) was stirred at room temperature for 1.25 h. The reaction mixture was then concentrated by rotary evaporation, dried under high vacuum to afford the title compound, which was used in the next step without further purification (38 mg, 0.045 mmol, 100% yield). ESI-MS: $C_{41}H_{47}N_{11}O_{10}$ (M + H), calcd 854.35; found, 854.20.

tert-Butyl (S)-4-((tert-Butoxycarbonyl)amino)-5-(((S)-1-(3-((5-carbamoyl-1-((E)-4-(5-carbamoyl-2-(4-ethyl-2-methyloxazole-5-carboxamido)-7-methoxy-1H-benzo[d]imidazole-1-yl)but-2-en-1-yl)-2-(4-ethyl-2-methyloxazole-5-carboxamido)-1H-benzo[d]-imidazole-7-yl)oxy)propoxy)-1-oxopropan-2-yl)amino)-5-oxopentanoate. (*E*)-3-((5-Carbamoyl-1-(4-(5-carbamoyl-2-(4-ethyl-2-methyloxazole-5-carboxamido)-7-methoxy-1*H*-benzo[*d*]imidazole-1-yl)-but-2-en-1-yl)-2-(4-ethyl-2-methyloxazole-5-carboxamido)-1*H*-benzo-[*d*]imidazole-7-yl)oxy)propyl L-alaninate (38 mg, 0.045 mmol), HOAt (6 mg, 0.045 mmol), (*S*)-5-(*tert*-butoxy)-2-((*tert*-butoxycarbonyl)amino)-5-oxopentanoic acid (14 mg, 0.045 mmol), HATU (26 mg, 0.068 mmol), and DMF (1.8 mL) were stirred at room temperature for 1.5 h. The reaction mixture was then diluted with DCM and adsorbed onto silica gel. Purification over silica gel afforded the title compound (51 mg, 0.045 mmol, 100% yield). ESI-MS: $C_{55}H_{70}N_{12}O_{15}$ (M + H), calcd 1139.51; found, 1139.31.

(S)-4-Amino-5-(((S)-1-(3-((5-carbamoyl-1-((E)-4-(5-carbamoyl-2-(4-ethyl-2-methyloxazole-5-carboxamido)-7-methoxy-1H-benzo-[d]imidazole-1-yl)but-2-en-1-yl)-2-(4-ethyl-2-methyloxazole-5-carboxamido)-1H-benzo[d]imidazole-7-yl)oxy)propoxy)-1-oxopropan-2-yl)amino)-5-oxopentanoic Acid. To a solution of *tert*-butyl (S)-4-((*tert*-butoxycarbonyl)amino)-5-(((S)-1-(3-((5-carbamoyl-1-((*E*)-4-(5-carbamoyl-2-(4-ethyl-2-methyloxazole-5-carboxamido)-7-methoxy-1*H*-benzo[*d*]imidazole-1-yl)but-2-en-1-yl)-2-(4-ethyl-2-methyloxazole-5-carboxamido)-1*H*-benzo[*d*]imidazole-7-yl)oxy)-propoxy)-1-oxopropan-2-yl)amino)-5-oxopentanoate (51 mg, 0.045 mmol) in DCM (0.895 mL) was charged TFA (0.895 mL), and the mixture was stirred at room temperature for 3 h. The reaction mixture was then concentrated by rotary evaporation and dried under high vacuum to afford the title compound, which was used in the next step without further purification (44 mg, 0.045 mmol, 100% yield). ESI-MS: $C_{46}H_{54}N_{12}O_{13}$ (M + H), calcd 983.39; found, 983.21.

(S)-5-(((S)-1-(3-((5-Carbamoyl-1-((E)-4-(5-carbamoyl-2-(4-ethyl-2-methyloxazole-5-carboxamido)-7-methoxy-1H-benzo[d]-imidazole-1-yl)but-2-en-1-yl)-2-(4-ethyl-2-methyloxazole-5-carboxamido)-1H-benzo[d]imidazole-7-yl)oxy)propoxy)-1-oxopropan-2-yl)amino)-4-(2-(2,5-dioxo-2,5-dihydro-1H-pyrrol-1-yl)-acetamido)-5-oxopentanoic Acid, Precursor to ADC ***43***. To a solution of (S)-4-amino-5-(((S)-1-(3-((5-carbamoyl-1-((*E*)-4-(5-carbamoyl-2-(4-ethyl-2-methyloxazole-5-carboxamido)-7-methoxy-1*H*-benzo[*d*]imidazole-1-yl)but-2-en-1-yl)-2-(4-ethyl-2-methyloxazole-5-carboxamido)-1*H*-benzo[*d*]imidazole-7-yl)oxy)propoxy)-1-oxopropan-2-yl)amino)-5-oxopentanoic acid (44 mg, 0.045 mmol) in DMF (1.3 mL) was charged (2,5-dioxopyrrolidin-1-yl 2-(2,5-dioxo-2,5-

https://doi.org/10.1021/acs.jmedchem.3c00907
J. Med. Chem. 2023, 66, 10715−10733

dihydro-1*H*-pyrrol-1-yl)acetate (13 mg, 0.052 mmol) and then D*i*PEA (0.5 mL, 2.97 mmol). The reaction was stirred at room temperature for 15 min and then quenched with the addition of AcOH (0.4 mL). The reaction mixture was filtered and then purified over silica gel to afford the title compound (17.5 mg, 0.016 mmol, 34.7% yield). ^{1}H NMR (400 MHz, DMSO-d_6): δ 12.68 (s, 1H), 8.41 (d, J = 6.8 Hz, 1H), 8.35 (d, J = 8.2 Hz, 1H), 7.91 (s, 2H), 7.62 (s, 2H), 7.30 (s, 3H), 7.06 (s, 2H), 5.85−5.66 (m, 3H), 4.88 (dd, J = 15 Hz, J = 4.3 Hz, 4H), 4.34−4.28 (m, 1H), 4.28−4.20 (m, 1H), 4.16−4.00 (m. 6H), 3.75 (s, 3H), 2.82−2.71 (m, 4H), 2.37 (s, 3H), 2.39−2.36 (m, 6H), 2.22 (t, J = 7.9 Hz, 3H), 1.92−1.82 (m, 3H), 1.76−1.63 (m, 2H), 1.24 (d, J = 7.9 Hz, 3H), 1.04−0.91 (m, 6H); ESI-MS: $C_{52}H_{57}N_{13}O_{16}$ (M + H), calcd 1120.40; found, 1120.38.

Precursors to ADC **44**, **45**, and **46** were prepared in a similar fashion as described above. The precursor to ADC **48** was prepared similar to the above, except for starting with **19b**.

(R)-5-(((S)-1-(3-((5-Carbamoyl-1-((E)-4-(5-carbamoyl-2-(4-ethyl-2-methyloxazole-5-carboxamido)-7-methoxy-1H-benzo[d]-imidazole-1-yl)but-2-en-1-yl)-2-(4-ethyl-2-methyloxazole-5-carboxamido)-1H-benzo[d]imidazole-7-yl)oxy)propoxy)-1-oxopropan-2-yl)amino)-4-(2-(2,5-dioxo-2,5-dihydro-1H-pyrrol-1-yl)-acetamido)-5-oxopentanoic Acid, Precursor to ADC **44**. $C_{52}H_{57}N_{13}O_{16}$ (M + H), calcd 1120.40; found, 1120.41.

(S)-5-(((R)-1-(3-((5-Carbamoyl-1-((E)-4-(5-carbamoyl-2-(4-ethyl-2-methyloxazole-5-carboxamido)-7-methoxy-1H-benzo[d]-imidazole-1-yl)but-2-en-1-yl)-2-(4-ethyl-2-methyloxazole-5-carboxamido)-1H-benzo[d]imidazole-7-yl)oxy)propoxy)-1-oxopropan-2-yl)amino)-4-(2-(2,5-dioxo-2,5-dihydro-1H-pyrrol-1-yl)-acetamido)-5-oxopentanoic Acid, Precursor to ADC **45**. ^{1}H NMR (400 MHz, DMSO-d_6): δ 12.68 (s, 1H), 8.35−8.31 (m, 2H), 7.91 (s, 2H), 7.62 (s, 2H), 7.30 (s, 3H), 7.04 (s, 2H), 5.85−5.66 (m, 3H), 4.88 (d, J = 15 Hz, 4H), 4.34−4.28 (m, 1H), 4.27−4.20 (m, 1H), 4.16−4.02 (m, 6H), 3.75 (s, 3H), 2.83−2.73 (m, 4H), 2.39−2.35 (m, 6H); 2.24−2.13 (m, 3H), 1.94−1.79 (m, 3H), 1.77−1.63 (m, 2H), 1.24 (d, J = 5 Hz, 3H), 1.01−0.92 (m, 6H). ESI-MS: $C_{52}H_{57}N_{13}O_{16}$ (M + H), calcd 1120.40; found, 1120.37.

(R)-5-(((R)-1-(3-((5-Carbamoyl-1-((E)-4-(5-carbamoyl-2-(4-ethyl-2-methyloxazole-5-carboxamido)-7-methoxy-1H-benzo[d]-imidazole-1-yl)but-2-en-1-yl)-2-(4-ethyl-2-methyloxazole-5-carboxamido)-1H-benzo[d]imidazole-7-yl)oxy)propoxy)-1-oxopropan-2-yl)amino)-4-(2-(2,5-dioxo-2,5-dihydro-1H-pyrrol-1-yl)-acetamido)-5-oxopentanoic Acid, Precursor to ADC **46**. ESI-MS: $C_{52}H_{57}N_{13}O_{16}$ (M + H), calcd 1120.40; found, 1120.11.

(S)-5-(((S)-1-(3-((5-Carbamoyl-1-((E)-4-(6-carbamoyl-2-(4-ethyl-2-methyloxazole-5-carboxamido)-3H-imidazo[4,5-b]pyridin-3-yl)-but-2-en-1-yl)-2-(4-ethyl-2-methyloxazole-5-carboxamido)-1H-benzo[d]imidazole-7-yl)oxy)propoxy)-1-oxopropan-2-yl)amino)-4-(2-(2,5-dioxo-2,5-dihydro-1H-pyrrol-1-yl)acetamido)-5-oxopentanoic Acid, Precursor to ADC **48**. ESI-MS: $C_{50}H_{54}N_{14}O_{15}$ (M + H), calcd 1091.39; found, 1091.21.

Preparation of STING Agonist ADCs. STING-agonist ADCs were generated by conjugating maleimide-containing scaffold-payload to native cysteines exposed by reduction of interchain disulfides.

Antibodies were reduced at 5 mg/mL in 50 mM HEPES, 1 mM EDTA, pH7 using 3 to 5 equiv of TCEP-HCl and reacted for 90 min at 37 °C. Maleimide-containing scaffold-payloads were solubilized in *N*,*N*-dimethylacetamide (Sigma 185884) and then 8 to 10 molar equivalents were added to the reduced antibodies for a final reaction concentration of 9% *N*,*N*-dimethylacetamide and incubated for 60 min at 37 °C. The conjugations were quenched with 15 molar equivalents of L-cysteine for 45 min at room temperature. Crude ADCs were purified by either six iterative rounds of ultrafiltration/dilution using a centrifugal concentrator with a 30 kDa MWCO (Millipore UFC903008) or by ceramic hydroxyapatite resin (CHT type II 40 μm, Bio-Rad 1584200). For CHT purification, the crude reactions were loaded using 10 mM sodium phosphate and eluted with 10 mM sodium phosphate and 2 M sodium chloride. Final ADCs were formulated and analyzed.

Final ADCs were tested by SEC, HIC, and UV−vis. Drug-to-antibody ratios were determined by UV−vis using the previously described method[26] using a NanoDrop2000 (Thermo Scientific) and measuring absorbance at 280 and 320 nm. SEC was tested on a TSKgel G3000SWXL (5 μm, 7.8 mm × 300 mm, Tosoh Bioscience) at 35 °C using isocratic conditions at a flow rate of 0.75 mL/min for 25 min (mobile phase 25 mmol/L sodium phosphate, 150 mmol/L sodium chloride). HIC was performed on a TSKgel Butyl-NPR column (2.5 μm, 4.6 mm × 100 mm, Tosoh Bioscience PN: 0042168) at 35 °C and eluted with a 25 min gradient from 0 to 100% B at a flow rate of 1 mL/min (mobile phase A: 1.5 mol/L ammonium sulfate in 25 mmol/L sodium phosphate, pH 7; mobile phase B: 25 mmol/L sodium phosphate, pH 7, 10% isopropanol).

Biological Evaluation. *Activation of Human STING Signaling in Permeabilized THP1 Cells.* THP1-Dual cells (NF-κB-SEAP and IRF-Lucia luciferase reporter monocytes, InvivoGen) (4×10^5 cells/well) were incubated with test compounds in 6-fold titration steps from 100 μM to 0.36 nM in permeabilized buffer (50 mM HEPES pH 7.0, 100 mM KCl, 3 mM $MgCl_2$, 85 mM sucrose, 0.2% BSA, 1 mM ATP, 0.1 mM GTP, 0.1 mM TTP, 1 μg/mL digitonin) for 30 min on ice. Cells were then washed and incubated in a fresh RPMI medium with 10% FBS at 37 °C with 5% CO_2 for 24 h. To evaluate IRF3 reporter levels, the cell culture supernatant (20 μL) from each incubated sample was added to QUANTI-Luc assay solution (InvivoGen, 50 μL), and the luminescence was measured with a SpectraMax M3 spectrophotometer (Molecular Devices).

SKOV3/THP1 IRF3 Reporter Cell Assay. For cancer and THP1 IRF3 reporter co-culture assay, SKOV3 cancer cells were seeded in 96-well tissue culture plates (∼15,000 cells/well) and allowed to attach overnight. Culture medium was replaced with assay medium (RPMI-1640, 10% FBS, 1% penicillin/streptomycin) and after adding the indicated test articles, the plates were incubated for 20 min at 37 °C. THP1 Dual IRF3 reporter cells (50,000 cells/well) were added and the plates incubated for 24 h at 37 °C with 5% CO_2. Supernatants were assayed for luciferase activity using ANTI-Luc luminescence assay reagent (InvivoGen, Cat# rep-qlc) on a SpectraMax M5 plate reader. Dose−response curves for all assays were generated using Graphpad Prism software. EC_{50} values were determined from the four-parameter curve fitting in GraphPad Prism.

Cytokine Analysis in Co-Culture Assay. Cytokine analysis in cell culture supernatants was performed with a Duo Set ELISA kit for CXCL10 from R&D Systems (Cat no. DY266) as per the manufacturer's recommendations. Dose−response curves were generated using GraphPad Prism software. EC_{50} values were determined from four-parameter curve fitting.

In Vivo Studies. All animal experiments were approved by and performed in accordance with the Institutional Animal Care and Use Committee protocols at the following research facilities: Charles River Discovery Services (North Carolina, USA) and Covance Laboratories Inc. (New Jersey, USA).

Anti-Tumor Activity Studies. Female CB.17 SCID mice (CB17/Icr-PrkdcSCID/IcoIcrCrl, Charles River) were subcutaneously inoculated in the right flank with 1×10^7 cells in 50% Matrigel (BD Biosciences). Animals were randomized into treatment groups when tumors reached a mean of 60−100 mm^3 and were administered a single, intravenous injection of the ADCs tested. Tumors were measured by caliper twice weekly and tumor volumes were calculated using the formula: width^2 × length/2.

In Vivo PK Studies in Mice. Female BALB/c (Figure 5) or CB.17 SCID (Figure 8) mice (n = 5) were administered a single, intravenous injection of the ADCs tested. Plasma was serially collected from each animal at various timepoints over 1−2 weeks.

Neat plasma was diluted 10-fold in micro-sampling stabilizer buffer prior to assay for the conjugated drug by LCMS and total antibody by ligand-binding assay. PK data were analyzed with Phoenix 8.3, and PK concentration−time profiles were presented by analyte and test articles. The limit of quantification (LOQ) for each analyte is as follows: total antibody for **47** and **48** = 9.14 ng/mL; conjugated drug for **47** and **48** = 35.1 and 33.5 ng/mL, respectively.

In Vivo Study of Non-Human Primates. A study in naïve cynomolgus monkeys was conducted to evaluate STING agonist ADCs at a matched antibody dose of 9 mg/kg administered via 45 min IV infusion (1 male/1 female per group). PK data for total mAb, conjugated drug, and free payload are shown in Figure 8D. LOQ for

https://doi.org/10.1021/acs.jmedchem.3c00907
J. Med. Chem. 2023, 66, 10715−10733

each analyte is as follows: total antibody for **47** and **48** = 9.14 ng/mL; conjugated drug for **47** and **48** = 3.19 and 5.37 ng/mL, respectively; free drug for **47** and **48** = 0.1 ng/mL. Key hematology data at 24 h are shown in Figure 8E.

■ ASSOCIATED CONTENT

Supporting Information

The Supporting Information is available free of charge at https://pubs.acs.org/doi/10.1021/acs.jmedchem.3c00907.

Co-crystal structure of human STING with bound **19b**, SPR analysis of select compounds, in vitro and in vivo PK parameters of **19b**, HIC traces for ADCs **36**-**40**, effect on mouse body weight after dosing of ADCs **37** and **42**, analytical characterization of ADCs **47** and **48**, and HPLC traces for lead compounds (PDF)

Molecular formula strings and the associated biological data (CSV)

Accession Codes

PDB ID for hSTING with bound **15** is 8STH. PDB ID for hSTING with bound **19b** is 8STI.

■ AUTHOR INFORMATION

Corresponding Author

Jeremy R. Duvall − *Mersana Therapeutics, Inc., Cambridge, Massachusetts 02139, United States;* orcid.org/0009-0004-9897-7924; Phone: +1 (617) 844-8542; Email: jduvall@mersana.com

Authors

Joshua D. Thomas − *Mersana Therapeutics, Inc., Cambridge, Massachusetts 02139, United States;* orcid.org/0000-0003-2974-8226

Raghida A. Bukhalid − *Mersana Therapeutics, Inc., Cambridge, Massachusetts 02139, United States*

Kalli C. Catcott − *Mersana Therapeutics, Inc., Cambridge, Massachusetts 02139, United States;* orcid.org/0000-0003-1941-0678

Keith W. Bentley − *Mersana Therapeutics, Inc., Cambridge, Massachusetts 02139, United States*

Scott D. Collins − *Mersana Therapeutics, Inc., Cambridge, Massachusetts 02139, United States*

Timothy Eitas − *Mersana Therapeutics, Inc., Cambridge, Massachusetts 02139, United States*

Brian D. Jones − *Mersana Therapeutics, Inc., Cambridge, Massachusetts 02139, United States*

Eugene W. Kelleher − *Mersana Therapeutics, Inc., Cambridge, Massachusetts 02139, United States*

Kelly Lancaster − *Mersana Therapeutics, Inc., Cambridge, Massachusetts 02139, United States*

Marina Protopopova − *Mersana Therapeutics, Inc., Cambridge, Massachusetts 02139, United States*

Soumya S. Ray − *3-Dimensional Consulting, Quincy, Massachusetts 02170, United States*

Elena Ter-Ovanesyan − *Mersana Therapeutics, Inc., Cambridge, Massachusetts 02139, United States*

Ling Xu − *Mersana Therapeutics, Inc., Cambridge, Massachusetts 02139, United States*

Liping Yang − *Mersana Therapeutics, Inc., Cambridge, Massachusetts 02139, United States*

Jeffrey Zurita − *Mersana Therapeutics, Inc., Cambridge, Massachusetts 02139, United States*

Marc Damelin − *Mersana Therapeutics, Inc., Cambridge, Massachusetts 02139, United States*

Dorin Toader − *Mersana Therapeutics, Inc., Cambridge, Massachusetts 02139, United States*

Timothy B. Lowinger − *Mersana Therapeutics, Inc., Cambridge, Massachusetts 02139, United States*

Complete contact information is available at: https://pubs.acs.org/10.1021/acs.jmedchem.3c00907

Author Contributions

All authors have given approval to the final version of the manuscript.

Notes

The authors declare the following competing financial interest(s): All authors except S.R. are or were employees and securityholders of Mersana Therapeutics, Inc.

■ ACKNOWLEDGMENTS

The authors wish to thank Winnie Lee, Travis Monnell, Dongmei Xiao, and Qingxiu Zhang for biology support; Ronald Eydelloth for toxicology consultations; Steve Bradley for supporting analytical characterization of reagents in PK studies; Radha Iyengar, Anouk Dirksen, Katsu Ishida, and Dian Su for helpful discussions; the team at Aurigene for chemistry support; and the team at Proteros for co-crystallization studies.

■ ABBREVIATIONS

DCC, dicyclohexylcarbodiimide; DCM, dichloromethane; DIPEA, *N*,*N*-diisopropylethylamine; DMAP, 4-dimethylaminopyridine; DMF, dimethylformamide; DMSO, dimethylsulfoxide; EDCI, 1-ethyl-3-(3-dimethylaminopropyl)carbodiimide; HATU, hexafluorophosphate azabenzotriazole tetramethyl uronium; HOAT, 1-hydroxy-7-azabenzotriazole; HOBT, 1-hydroxybenzotriazole; PyBOP, benzotriazol-1-yl-oxytripyrrolidinophosphonium hexafluorophosphate; TCEP, tris(2-carboxyethyl)phosphine; TFA, trifluoroacetic acid; THF, tetrahydrofuran; TLC, thin-layer chromatography

■ REFERENCES

(1) Chen, D.; Mellman, I. Elements of cancer immunity and the cancer−immune set point. *Nature* **2017**, *541*, 321−330.

(2) Trujillo, J. A.; Sweis, R. F.; Bao, R.; Luke, J. J. T Cell−Inflamed versus Non-T Cell−Inflamed Tumors: A Conceptual Framework for Cancer Immunotherapy Drug Development and Combination Therapy Selection. *Cancer Immunol. Res.* **2018**, *6*, 990−1000.

(3) Akira, S.; Uematsu, S.; Takeuchi, O. Pathogen recognition and innate immunity. *Cell* **2006**, *124*, 783−801.

(4) Demaria, O.; Cornen, S.; Daëron, M.; Morel, Y.; Medzhitov, R.; Vivier, E. Harnessing innate immunity in cancer therapy. *Nature* **2019**, *574*, 45−56.

(5) Corrales, L.; Glickman, L. H.; McWhirter, S. M.; Kanne, D. B.; Sivick, K. E.; Katibah, G. E.; Woo, S.-R.; Lemmens, E.; Banda, T.; Leong, J. J.; Metchette, K.; Dubensky, T. W., Jr.; Gajewski, T. F. Direct activation of STING in the tumor microenvironment leads to potent and systemic tumor regression and immunity. *Cell Rep.* **2015**, *11*, 1018−1030.

(6) Ramanjulu, J. M.; Pesiridis, G. S.; Yang, J.; Concha, N.; Singhaus, R.; Zhang, S.-Y.; Tran, J.-L.; Moore, P.; Lehmann, S.; Eberl, H. C.; Muelbaier, M.; Schneck, J. L.; Clemens, J.; Adam, M.; Mehlmann, J.; Romano, J.; Morales, A.; Kang, J.; Leister, L.; Graybill, T. L.; Charnley, A. K.; Ye, G.; Nevins, N.; Behnia, K.; Wolf, A. I.; Kasparcova, V.; Nurse, K.; Wang, L.; Puhl, A. C.; Li, Y.; Klein, M.; Hopson, C. B.; Guss, J.; Bantscheff, M.; Bergamini, G.; Reilly, M. A.; Lian, Y.; Duffy, K. J.; Adams, J.; Foley, K. P.; Gough, P. J.; Marquis, R. W.; Smothers, J.; Hoos, A.; Bertin, J. Design of amidobenzimidazole

STING receptor agonists with systemic activity. *Nature* **2018**, *564*, 439−443.
(7) Meric-Bernstam, F.; Sweis, R. F.; Hodi, F. S.; Messersmith, W. A.; Andtbacka, R. H. I.; Ingham, M.; Lewis, N.; Chen, X.; Pelletier, M.; Chen, X.; Wu, J.; Dubensky, T. W.; McWhirter, S. M.; Müller, T.; Nair, N.; et al. Phase I dose-escalation trial of MIW815 (ADU-S100), an intratumoral STING agonist, in patients with advanced/metastatic solid tumors or lymphomas. *Clin. Cancer Res.* **2022**, *28*, 677−688.
(8) Pillow, T. H.; Adhikari, P.; Blake, R. A.; Chen, J.; Del Rosario, G.; Deshmukh, G.; Figueroa, I.; Gascoigne, K. E.; Kamath, A. V.; Kaufman, S.; Kleinheinz, T.; Kozak, K. R.; Latifi, B.; Leipold, D. D.; Sing Li, C.; Li, R.; Mulvihill, M. M.; O'Donohue, A.; Rowntree, R. K.; Sadowsky, J. D.; Wai, J.; Wang, X.; Wu, C.; Xu, Z.; Yao, H.; Yu, S.-F.; Zhang, D.; Zang, R.; Zhang, H.; Zhou, H.; Zhu, X.; Dragovich, P. S. Antibody conjugation of a chimeric BET degrader enables in vivo activity. *ChemMedChem* **2020**, *15*, 17−25.
(9) Fang, S.; Brems, B. M.; Olawode, E. O.; Miller, J. T.; Brooks, T. A.; Tumey, L. N. Design and characterization of immune-stimulating imidazo[4,5-c]quinoline antibody-drug conjugates. *Mol. Pharmacol.* **2022**, *19*, 3228−3241.
(10) He, L.; Wang, L.; Wang, Z.; Li, T.; Chen, H.; Zhang, Y.; Hu, Z.; Dimitrov, D. S.; Du, J.; Liao, X. Immune modulating antibody−drug conjugate (IM-ADC) for cancer immunotherapy. *J. Med. Chem.* **2021**, *64*, 15716−15726.
(11) Ackerman, S. E.; Pearson, C. I.; Gregorio, J. D.; Gonzalez, J. C.; Kenkel, J. A.; Hartmann, F. J.; Luo, A.; Ho, P. Y.; LeBlanc, H.; Blum, L. K.; Kimmey, S. C.; Luo, A.; Nguyen, M. L.; Paik, J. C.; Sheu, L. Y.; Ackerman, B.; Lee, A.; Li, H.; Melrose, J.; Laura, R. P.; Ramani, V. C.; Henning, K. A.; Jackson, D. Y.; Safina, B. S.; Yonehiro, G.; Devens, B. H.; Carmi, Y.; Chapin, S. J.; Bendall, S. C.; Kowanetz, M.; Dornan, D.; Engleman, E. G.; Alonso, M. N. Immune-stimulating antibody conjugates elicit robust myeloid activation and durable antitumor immunity. *Nat. Cancer* **2021**, *2*, 18−33.
(12) Han, A.; Olsen, O.; D'Souza, C.; Shan, J.; Zhao, F.; Yanolatos, J.; Hovhannisyan, Z.; Haxhinasto, S.; Delfino, F.; Olson, W. Development of novel glucocorticoids for use in antibody−drug conjugates for the treatment of inflammatory diseases. *J. Med. Chem.* **2021**, *64*, 11958−11971.
(13) Lehar, S. M.; Pillow, T.; Xu, M.; Staben, L.; Kajihara, K. K.; Vandlen, R.; DePalatis, L.; Raab, H.; Hazenbos, W. L.; Hiroshi Morisaki, J.; Kim, J.; Park, S.; Darwish, M.; Lee, B.-C.; Hernandez, H.; Loyet, K. M.; Lupardus, P.; Fong, R.; Yan, D.; Chalouni, C.; Luis, E.; Khalfin, Y.; Plise, E.; Cheong, J.; Lyssikatos, J. P.; Strandh, M.; Koefoed, K.; Andersen, P. S.; Flygare, J. A.; Wah Tan, M.; Brown, E. J.; Mariathasan, S. Novel antibody−antibiotic conjugate eliminates intracellular *S. aureus*. *Nature* **2015**, *527*, 323−328.
(14) Bukhalid, R. A.; Duvall, J. R.; Lancaster, K.; Catcott, K. C.; Cetinbas, N. M.; Monnell, T.; Routhier, C.; Thomas, J. D.; Bentley, K. W.; Collins, S. D.; Ditty, E.; Eitas, T. K.; Kelleher, E. W.; Shaw, P.; Soomer-James, J.; Ter-Ovanesyan, E.; Xu, L.; Zurita, J.; Toader, D.; Damelin, M.; Lowinger, T. B. XMT-2056, a HER2-directed STING agonist antibody-drug conjugate, induces an innate anti-tumor immune response by acting on cancer cells and tumor-resident immune cells, **2023**. Manuscript in preparation.
(15) Goldenberg, D. M. Targeting of cancer with radiolabeled antibodies. Prospects for imaging and therapy. *Arch. Pathol. Lab. Med.* **1988**, *112*, 580−587.
(16) Hughes, B. Antibody-drug conjugates for cancer: poised to deliver? *Nat. Rev. Drug Discovery* **2010**, *9*, 665−667.
(17) Chari, R. V. J. Targeted cancer therapy: conferring specificity to cytotoxic drugs. *Acc. Chem. Res.* **2008**, *41*, 98−107.
(18) Lyon, R. P.; Bovee, T. D.; Doronina, S. O.; Burke, P. J.; Hunter, J. H.; Neff-LaFord, H. D.; Jonas, M.; Anderson, M. E.; Setter, J. R.; Senter, P. D. Reducing hydrophobicity of homogeneous antibody-drug conjugates improves pharmacokinetics and therapeutic index. *Nat. Biotechnol.* **2015**, *33*, 733−735.
(19) Zhang, X.; Shi, H.; Wu, J.; Zhang, X.; Sun, L.; Chen, C.; Chen, Z. J. Cyclic GMP-AMP containing mixed phosphodiester linkages is an endogenous high-affinity ligand for STING. *Mol. Cell* **2013**, *51*, 226−235.
(20) Gao, P.; Ascano, M.; Zillinger, T.; Wang, W.; Dai, P.; Serganov, A. A.; Gaffney, B. L.; Shuman, S.; Jones, R. A.; Deng, L.; Hartmann, G.; Barchet, W.; Tuschl, T.; Patel, D. J. Structure-function analysis of STING activation by c[G(2',5')pA(3',5')p] and targeting by antiviral DMXAA. *Cell* **2013**, *154*, 748−762.
(21) Song, Z.; Wang, X.; Zhang, Y.; Gu, W.; Shen, A.; Ding, C.; Li, H.; Xiao, R.; Geng, M.; Xie, Z.; Zhang, A. Structure−activity relationship study of amidobenzimidazole analogues leading to potent and systemically administrable stimulator of interferon gene (STING) agonists. *J. Med. Chem.* **2021**, *64*, 1649−1669.
(22) Lyon, R. P.; Setter, J. R.; Bovee, T. D.; Doronina, S. O.; Hunter, J. H.; Anderson, M. E.; Balasubramanian, C. L.; Duniho, S. M.; Leiske, C. I.; Li, F.; Senter, P. D. Self-hydrolyzing maleimides improve the stability and pharmacological properties of antibody-drug conjugates. *Nat. Biotechnol.* **2014**, *32*, 1059−1062.
(23) Burke, P. J.; Hamilton, J. Z.; Jeffrey, S. C.; Hunter, J. H.; Doronina, S. O.; Okeley, N. M.; Miyamoto, J. B.; Anderson, M. E.; Stone, I. J.; Ulrich, M. L.; Simmons, J. K.; McKinney, E. E.; Senter, P. D.; Lyon, R. P. Optimization of a PEGylated glucuronide-monomethylauristatin E linker for antibody-drug conjugates. *Mol. Cancer Ther.* **2017**, *16*, 116−123.
(24) Shao, T.; Chen, T.; Chen, Y.; Liu, X.; Chen, Y.-L.; Wang, Q.; Zhu, T.; Guo, M.; Li, H.; Ju, D.; Wang, C. Construction of paclitaxel-based antibody-drug conjugates with a PEGylated linker to achieve superior therapeutic index. *Signal Transduction Targeted Ther.* **2020**, *5*, 132.
(25) Su, D.; Kozak, K. R.; Sadowsky, J.; Yu, S.-F.; Fourie-O'Donohue, A.; Nelson, C.; Vandlen, R.; Ohri, R.; Liu, L.; Ng, C.; He, J.; Davis, H.; Lau, J.; Del Rosario, G.; Cosino, E.; Cruz-Chuh, J. d.; Ma, Y.; Zhang, D.; Darwish, M.; Cai, W.; Chen, C.; Zhou, H.; Lu, J.; Liu, Y.; Kaur, S.; Xu, K.; Pillow, T. H. Modulating antibody−drug conjugate payload metabolism by conjugation site and linker modification. *Bioconjugate Chem.* **2018**, *29*, 1155−1167.
(26) Hamblett, K. J.; Senter, P. D.; Chace, D. F.; Sun, M. M. C.; Lenox, J.; Cerveny, C. G.; Kissler, K. M.; Bernhardt, S. X.; Kopcha, A. K.; Zabinski, R. F.; Meyer, D.; et al. Effects of drug loading on the antitumor activity of a monoclonal antibody drug conjugate. *Clin. Cancer Res.* **2004**, *10*, 7063−7070.

https://doi.org/10.1021/acs.jmedchem.3c00907
J. Med. Chem. 2023, 66, 10715−10733